

# Correlation-consistency cartography of the double inflation landscape

Shinji Tsujikawa<sup>1</sup>, David Parkinson<sup>2</sup> and Bruce A. Bassett<sup>2</sup>

<sup>1</sup> *Research Center for the Early Universe, University of Tokyo, Hongo, Bunkyo-ku, Tokyo 113-0033, Japan*

<sup>2</sup> *Institute of Cosmology and Gravitation, University of Portsmouth, Mercantile House, Portsmouth PO1 2EG, United Kingdom*

(March 22, 2019)

We show explicitly some exciting general features of double-inflation: (i) they can often lead to strongly correlated adiabatic and entropy (isocurvature) power spectra. (ii) The two-field slow-roll consistency relations can be violated when the correlation is large at Hubble crossing. (iii) The resulting spectra of adiabatic and entropy perturbations can be strongly scale-dependent and tilted toward either the red or blue. These effects are typically due to a light or time-dependent entropy mass and a non-negligible angular velocity in field space during inflation. They are illustrated via a wide multi-parameter numerical search for correlations in two concrete models. The correlation is found to be particularly strong in a supersymmetric scenario due to rapid growth of entropy perturbations in the tachyonic region separating the two inflationary stages. Our analysis suggests that realistic double-inflation models will provide a rich and fruitful arena for the application of future cosmic data sets and new approximation schemes which go beyond slow-roll.

PACS 98.80.Cq

## I. INTRODUCTION

One of the radical developments in recent inflationary research has been the realisation – implicit in early work [1] – that inflationary predictions for the CMB and large-scale structure (LSS) can depend sensitively on post-inflationary, but pre-photon-decoupling, physics. This is a departure from the single-field inflationary paradigm [2] that has been the backbone of high-energy cosmology over the past 20 years. This rather subtle paradigm shift can be primarily attributed to the driving force of particle physics inflationary models [3] which necessarily involve more than one dynamically important field and often lead to more than one phase of inflation [4].

The key point about multi-field models of inflation for this paper is that they allow for substantial super-Hubble entropy/isocurvature perturbations [5] (see also refs. [6,7]). This implies a very interesting dynamics since, *at linear order*, entropy perturbations source adiabatic perturbations while the converse is not true in the large scale limit [8] (though see the counter-claims in [9]). Further, these entropy modes can be partially or completely correlated with the adiabatic modes, and this correlation <sup>1</sup> is both important for the CMB and sensitive to the way in which reheating occurs.

Our aim in this paper is to provide the first exhaustive study of adiabatic-entropy correlations in “realistic” double inflation models. Given that the current CMB data actually favour such a correlated cocktail [10] there exists the exciting possibility that upcoming data will allow us to significantly constrain realistic inflationary parameter spaces.

Let us briefly recap the areas discovered so far for which entropy perturbations can be important.

- *Perturbations in multi-field inflationary models* [11]- [34] – models with two or more phases of inflation typically lead to some correlation due to the curvature of the phase curves in field space. This correlation can be preserved or wiped-out depending on the precise details of reheating.
- *The curvaton* [35] - an entropy perturbation can be converted into an adiabatic perturbation with a total correlation.
- *Preheating* [36]- the non-perturbative, resonant, decay of the inflaton can affect standard inflationary predictions for the CMB in certain special cases where there is an entropy perturbation on large scales that is resonantly amplified at preheating.

---

<sup>1</sup>This mode-mode correlation is to be contrasted with the time-dependent correlations of [12].

The possibility of correlated mixtures of adiabatic and isocurvature perturbations is both exciting and depressing for phenomenology. Instead of a single (adiabatic) power spectrum, one needs a matrix of power spectra [37,38] describing the full correlation network for the complex cosmic cocktail of fluids. In addition the evolution of the correlation power spectra is very sensitive to the way in which particle decays occur after inflation. The precise nature of decay channels and widths during and after reheating can preserve or wash-out pre-existing correlations, introducing new arbitrary parameters but also opening up a new window on particle physics beyond the inflaton potential. Multi-field models may also lead to significant levels of non-Gaussianity in the CMB transferred from the entropy to adiabatic modes [39].

There are still unresolved issues in the multi-field context. In particular, the validity of the slow-roll approximation has not been fully explored. Indeed, this is one of the aims of our analysis. In addition, new effects occur in the case when the kinetic terms of the scalar fields are not canonical (e.g. nonlinear sigma model) and hence parametrise a curved manifold, as occurs in the case of scalar-tensor theories [15,16,32] and string-inspired cosmologies [40].

An analysis of scalar perturbations in such a general situation has been studied [16,20] but only under the assumption of the slow-roll. Even in the single-field case the slow-roll approximation can introduce errors in the calculation of the CMB spectrum of up to 15% [41] and going to higher order in the slow-roll parameters may be necessary [42]. The situation in the more general case is clearly more subtle.

Recently Bartolo *et al.* [31] investigated the spectra of correlated perturbations and the modification of the standard consistency relation,  $n_T = -2r_T$ , using the slow-roll analysis in the multi-field context (Here  $n_T$  is the spectral index of the gravitational wave and  $r_T$  is the relative amplitude of tensor to scalar perturbations). According to their results, the *single-field* consistency relation is significantly modified when the correlation of adiabatic and isocurvature perturbations is strong.

In addition to the standard roll-approximation where the second-order derivatives of scalar fields are neglected, Bartolo *et al.* assumed that the adiabatic/entropy mass and the scalar field velocity angle evolve slowly during the multiple phases of inflation. While the latter approximation is generally valid in the single-field context, this is not so in models with two stages of inflation because the masses of field perturbations as well as the slow-roll parameters already get large around the end of the *first* stage of inflation. More recently Wands *et al.* [34] rederived one of the consistency relations assuming slow-roll only *at* horizon crossing, whereas the other consistency relation requires slow-roll to be valid at all stages of inflation.

In this work we shall consider the more general situation where the slow-roll conditions are not necessarily satisfied even at horizon crossing and check the validity of the two consistency relations numerically in “realistic” double inflation models. The models we adopt are the double inflation with two massive scalar fields (both noninteracting [13,14,24] and interacting [18]) and the two-stage supersymmetric inflation with tachyonic (spinodal) instability [43,44,45] where the second derivative of the potential becomes negative.

The former model is probably the simplest double-inflation generalisation of the chaotic inflationary scenario. The second model is motivated by supersymmetric theories [46]- [51], in which case the potentials of scalar fields generically have tachyonic instability regions. Since these two kinds of models include the basic properties of double inflation, it is straightforward to extend our analysis to other double inflationary scenarios.

We organise our paper as follows. In Sec. II we present the general framework of our analysis including the multi-field decomposition into adiabatic and entropy field perturbations and the resulting power spectra of correlated density perturbations. We also discuss the limitation of the slow-roll approximation in the multi-field context. In Sec. III we analyze the model with two massive scalar fields. Sec. IV is devoted to the double inflation with a tachyonic instability while the final section concludes.

## II. GENERAL FRAMEWORK

Let us consider two-field inflation with minimally coupled scalar fields,  $\phi$  and  $\chi$ , with a potential  $V(\phi, \chi)$ . In a flat Friedmann-Lemaître-Robertson-Walker (FLRW) background with a scale factor  $a$ , the background equations are

$$H^2 \equiv \left(\frac{\dot{a}}{a}\right)^2 = \frac{\kappa^2}{3} \left(\frac{1}{2}\dot{\phi}^2 + \frac{1}{2}\dot{\chi}^2 + V\right), \quad \dot{H} = -\frac{\kappa^2}{2} (\dot{\phi}^2 + \dot{\chi}^2), \quad (2.1)$$

$$\ddot{\phi} + 3H\dot{\phi} + V_\phi = 0, \quad \ddot{\chi} + 3H\dot{\chi} + V_\chi = 0, \quad (2.2)$$

where  $V_\phi \equiv \partial V/\partial\phi$ ,  $H$  is the Hubble expansion rate, and  $\kappa^2 = 8\pi/M_p^2$  with  $M_p$  being the Planck mass. At linear order minimally coupled scalar fields do not induce an anisotropic stress [6,7,52] and hence scalar metric perturbations can be characterised by a single potential  $\Phi$ . The metric in longitudinal gauge then becomes:

$$ds^2 = -(1 + 2\Phi)dt^2 + a^2(1 - 2\Phi)\delta_{ij}dx^i dx^j. \quad (2.3)$$

The Fourier transformed, linearised Einstein equations for field and metric perturbations in this gauge are

$$\dot{\Phi} + H\Phi = \frac{\kappa^2}{2} (\dot{\phi}\delta\phi + \dot{\chi}\delta\chi), \quad (2.4)$$

$$\delta\ddot{\phi} + 3H\delta\dot{\phi} + \left(\frac{k^2}{a^2} + V_{\phi\phi}\right)\delta\phi = -2V_{\phi}\Phi + 4\dot{\phi}\dot{\Phi} - V_{\phi\chi}\delta\chi, \quad (2.5)$$

$$\delta\ddot{\chi} + 3H\delta\dot{\chi} + \left(\frac{k^2}{a^2} + V_{\chi\chi}\right)\delta\chi = -2V_{\chi}\Phi + 4\dot{\chi}\dot{\Phi} - V_{\phi\chi}\delta\phi, \quad (2.6)$$

where  $k$  is comoving momentum (wavenumber). All first order quantities in the equations that follow are functions of both  $k$  and  $t$  (the  $k$  subscript is implicit) <sup>2</sup>.

We now provide a self-contained review of the decomposition of adiabatic and isocurvature scalar field perturbations [8] and the resulting spectra of correlated perturbations [31]. These two papers are our basic references in this section and we will, where possible, follow their notation.

We will then also discuss the limitations of results obtained using slow-roll analysis.

Let us first introduce the ‘‘adiabatic’’ field,  $\sigma$ , and the ‘‘entropy’’ field,  $s$ , defined by

$$d\sigma = (\cos\theta)d\phi + (\sin\theta)d\chi, \quad ds = -(\sin\theta)d\phi + (\cos\theta)d\chi. \quad (2.7)$$

Here  $\theta$  is the angle of the trajectory in field space, satisfying  $\tan\theta = \dot{\chi}/\dot{\phi}$ . With an effective potential  $V(\phi, \chi)$ , the equations for adiabatic and entropy field perturbations are written in the form [8]

$$\delta\ddot{\sigma} + 3H\delta\dot{\sigma} + \left(\frac{k^2}{a^2} + V_{\sigma\sigma} - \dot{\theta}^2\right)\delta\sigma = -2V_{\sigma}\Phi + 4\dot{\sigma}\dot{\Phi} + 2(\dot{\theta}\delta s)^{\bullet} - \frac{2V_{\sigma}}{\dot{\sigma}}\dot{\theta}\delta s, \quad (2.8)$$

$$\delta\ddot{s} + 3H\delta\dot{s} + \left(\frac{k^2}{a^2} + V_{ss} + 3\dot{\theta}^2\right)\delta s = \frac{\dot{\theta}}{\dot{\sigma}} \frac{k^2}{2\pi G a^2} \Phi, \quad (2.9)$$

where

$$V_{\sigma\sigma} = (\cos^2\theta)V_{\phi\phi} + (\sin 2\theta)V_{\phi\chi} + (\sin^2\theta)V_{\chi\chi}, \quad (2.10)$$

$$V_{ss} = (\sin^2\theta)V_{\phi\phi} - (\sin 2\theta)V_{\phi\chi} + (\cos^2\theta)V_{\chi\chi}. \quad (2.11)$$

From eq. (2.4) we have

$$\Phi = \frac{\kappa^2}{2a} \int a\dot{\sigma}\delta\sigma dt. \quad (2.12)$$

This indicates that the gravitational potential is sourced by the adiabatic field perturbation.

Introducing the Sasaki-Mukhanov variable [53]

$$Q_{\sigma} \equiv \delta\sigma + \frac{\dot{\sigma}}{H}\Phi, \quad (2.13)$$

the equation for the adiabatic field perturbation can be rewritten as [8]

$$\ddot{Q}_{\sigma} + 3H\dot{Q}_{\sigma} + \left[\frac{k^2}{a^2} + V_{\sigma\sigma} - \dot{\theta}^2 - \frac{\kappa^2}{a^3} \left(\frac{a^3\dot{\sigma}^2}{H}\right)^{\bullet}\right] Q_{\sigma} = 2(\dot{\theta}\delta s)^{\bullet} - 2\left(\frac{V_{\sigma}}{\dot{\sigma}} + \frac{\dot{H}}{H}\right)\dot{\theta}\delta s. \quad (2.14)$$

The slow-roll solutions for  $Q_{\sigma}$  and  $\delta s$  can be obtained by neglecting the second-order derivatives ( $\ddot{Q}_{\sigma}$  and  $\delta\ddot{s}$ ) in eqs. (2.14) and (2.9). The evolution of fluctuations using this slow-roll approximation shows fairly good agreement

---

<sup>2</sup>In this paper we will often use the phrase ‘‘horizon crossing’’. This should be read ‘‘Hubble radius crossing’’ occurring for a mode with wavenumber  $k$  when  $k = aH$ .

with numerical results except around the end of inflation [32] unless there exists an intermediate non-inflationary stage (see ref. [13]). Other kinds of slow-roll approximations discussed later are more problematic however.

Note, however, that neglecting the second-order derivatives in eqs. (2.14) and (2.9) still leads to deviation of the power spectra at the *end* of inflation as found in numerical simulations in ref. [32]. In this work, we numerically follow the evolution of perturbations during double inflation and estimate the spectra right after the end of inflation.

To provide the comparison to our full numerical results consider the solutions for eqs. (2.14) and (2.9), found by neglecting  $\ddot{Q}_\sigma$  and  $\delta\dot{s}$  [31]. These solutions correspond to neglecting the decaying modes of  $Q_\sigma$  and  $\delta s$ . Then one has

$$Q_\sigma \simeq Af(t) + BP(t), \quad \delta s \simeq Bg(t). \quad (2.15)$$

Here  $A = A(k)$  and  $B = B(k)$ . When  $f = g = 1$  and  $P = 0$  at horizon crossing ( $k = aH$ ) the amplitudes  $A$  and  $B$  are determined by the quantum fluctuations within the Hubble radius:

$$A = \frac{H_k}{\sqrt{2k^3}} e_Q(\mathbf{k}), \quad B = \frac{H_k}{\sqrt{2k^3}} e_s(\mathbf{k}). \quad (2.16)$$

Here  $e_Q(\mathbf{k})$  and  $e_s(\mathbf{k})$  are classical stochastic Gaussian quantities, satisfying  $\langle e_Q(\mathbf{k}) \rangle = \langle e_s(\mathbf{k}) \rangle = 0$  and  $\langle e_i(\mathbf{k}) e_j^*(\mathbf{k}') \rangle = \delta_{ij} \delta^{(3)}(\mathbf{k} - \mathbf{k}')$ . Note that  $H_k$  is the Hubble parameter at horizon crossing. We caution the reader that in the context of double inflation  $P$  can be nonzero at horizon crossing due to strong correlations. Clearly then the assumption of uncorrelated adiabatic and entropy perturbations at  $k = aH$  are not generally justified. In order to make an accurate numerical analysis we choose the Bunch-Davies vacuum state deep inside the horizon ( $k \gg aH$ ) so that the  $\dot{\theta}$  term in the rhs of eq. (2.14) is negligible initially.

On super-Hubble scales ( $k \ll aH$ ) the slow-roll solution for  $\delta s$  can be written as

$$g(t) = \exp\left(-\int_{N(t)}^{N_k} \frac{\mu_s^2}{3H^2} dN\right) \simeq \exp\left[-\frac{\mu_s^2}{3H^2} (N_k - N(t))\right], \quad (2.17)$$

where  $\mu_s^2 \equiv V_{ss} + 3\dot{\theta}^2$  and  $N(t) = -\int_{t_f}^t H dt$  with  $t_f$  being the time at the end of inflation. The quantity,  $N_k = -\int_{t_f}^{t_k} H dt$ , corresponds to the e-folding between the horizon crossing and the end of inflation.

In deriving eq. (2.17) the time-dependence of the  $-\mu_s^2/(3H^2)$  term has been neglected, and this term is pulled out of the integral. In the single-field inflationary scenario, the variation of this term is associated with the end of inflation, in which case the error in this approximation is not significant for cosmologically relevant scales. In the case of double inflation, the situation is quite different. Since the mass term  $-\mu_s^2/(3H^2)$  already grows large at the end of the *first* stage of inflation, the assumption that the value of  $-\mu_s^2/(3H^2)$  will not change during *both* stages of inflation is not generally valid. In fact we shall numerically show later that this term typically changes significantly during double-inflation. This casts doubts on results derived using this approximation and suggests that a more sophisticated approximation may be needed to handle multiple phases of inflation completely.

The slow-roll expansion for  $-\mu_s^2/(3H^2)$  is given as [31]

$$-\frac{\mu_s^2}{3H^2} = -\frac{\epsilon_\chi \eta_{\phi\phi} + \epsilon_\phi \eta_{\chi\chi}}{\epsilon_t} + 2 \frac{(\pm\sqrt{\epsilon_\phi})(\pm\sqrt{\epsilon_\chi})}{\epsilon_t} \eta_{\phi\chi}, \quad (2.18)$$

where the slow-roll parameters are defined by

$$\epsilon_I \equiv \frac{1}{2\kappa^2} \left(\frac{V_{\phi_I}}{V}\right)^2, \quad \eta_{IJ} \equiv \frac{1}{\kappa^2} \frac{V_{\phi_I \phi_J}}{V}, \quad (2.19)$$

with  $\epsilon_t \equiv \epsilon_\phi + \epsilon_\chi$ . The entropy field perturbation at the end of inflation is approximately expressed as eq. (2.17) with

$$g(t_f) = \exp\left[\left(-\frac{\epsilon_\chi \eta_{\phi\phi} + \epsilon_\phi \eta_{\chi\chi}}{\epsilon_t} + 2 \frac{(\pm\sqrt{\epsilon_\phi})(\pm\sqrt{\epsilon_\chi})}{\epsilon_t} \eta_{\phi\chi}\right)_k N_k\right], \quad (2.20)$$

where we set  $N(t_f) = 0$ . The slow-roll parameters in this expression is evaluated at horizon crossing,  $k = aH$ , since the constancy of the mass term is assumed in eq. (2.17) [the subscript “ $k$ ” in eq. (2.20) denotes the value at horizon crossing].

The slow-roll solution for  $Q_\sigma$  at the end of inflation can be obtained by assuming the constancy of  $\mu_Q^2/H^2 \equiv (V_{\sigma\sigma} - \dot{\theta}^2 - \kappa^2 a^{-3}(a^3 \dot{\sigma}^2/H)^\bullet)/H^2$  and  $\dot{\theta}/H$ , as

$$f(t_f) = \exp \left[ \left( -\frac{\epsilon_\chi \eta_{\chi\chi} + \epsilon_\phi \eta_{\phi\phi}}{\epsilon_t} - 2 \frac{(\pm\sqrt{\epsilon_\phi})(\pm\sqrt{\epsilon_\chi})}{\epsilon_t} \eta_{\phi\chi} + 2\epsilon_t \right) N_k \right], \quad P(t_f) = 2g(t_f) \left( \frac{\dot{\theta}}{H} \right)_k \frac{e^{\zeta_k N_k} - 1}{\zeta_k}, \quad (2.21)$$

where

$$\zeta \equiv \frac{\mu_s^2 - \mu_Q^2}{3H^2} = \frac{(\epsilon_\phi - \epsilon_\chi)(\eta_{\chi\chi} - \eta_{\phi\phi})}{\epsilon_t} - 4 \frac{(\pm\sqrt{\epsilon_\phi})(\pm\sqrt{\epsilon_\chi})}{\epsilon_t} \eta_{\phi\chi} + 2\epsilon_t, \quad (2.22)$$

and

$$\frac{\dot{\theta}}{H} = \frac{\epsilon_\phi - \epsilon_\chi}{\epsilon_t} \eta_{\phi\chi} + \frac{(\pm\sqrt{\epsilon_\phi})(\pm\sqrt{\epsilon_\chi})}{\epsilon_t} (\eta_{\phi\phi} - \eta_{\chi\chi}). \quad (2.23)$$

In eq. (2.21)  $\zeta_k$  and  $(\dot{\theta}/H)_k$  are evaluated at horizon crossing due to the assumption of time-independence during inflation. This assumption is not generally justified in the context of the double inflation, as we already mentioned.

The curvature perturbation,  $\mathcal{R}$ , is defined by [8]

$$\mathcal{R} \equiv \Phi + H \frac{\dot{\phi}\delta\phi + \dot{\chi}\delta\chi}{\dot{\phi}^2 + \dot{\chi}^2} = \frac{H}{\dot{\sigma}} Q_\sigma. \quad (2.24)$$

Since the time-derivative of  $\mathcal{R}$  is given as [53,8]

$$\dot{\mathcal{R}} = \frac{H}{\dot{H}} \frac{k^2}{a^2} \Phi + \frac{2H}{\dot{\sigma}} \dot{\theta} \delta s, \quad (2.25)$$

the curvature perturbation is not conserved even in the large-scale limit ( $k \rightarrow 0$ ) in the presence of the entropy field perturbation,  $\delta s$ . Therefore the constancy of  $\mathcal{R}$  that is typically assumed in the slow-roll single-field inflationary scenario is not valid in the multi-field case. Instead we need to estimate the power spectrum of  $\mathcal{R}$  at the end of inflation from eq. (2.15), as

$$\mathcal{P}_{\mathcal{R}} = \left( \frac{H_k}{2\pi} \right)^2 \frac{H^2(t_f)}{\dot{\sigma}^2(t_f)} [|f^2(t_f)| + |P^2(t_f)|] \simeq \frac{1}{\pi} \left( \frac{H_k}{M_p} \right)^2 \frac{1}{\epsilon_t(t_f)} [|f^2(t_f)| + |P^2(t_f)|]. \quad (2.26)$$

The isocurvature perturbation of two scalar fields  $\chi$  and  $\phi$  is defined by [6]

$$S_{\chi\phi} \equiv \frac{\delta\rho_\chi}{\rho_\chi + p_\chi} - \frac{\delta\rho_\phi}{\rho_\phi + p_\phi} = \dot{\delta}_{\chi\phi} - 3H\delta_{\chi\phi}, \quad (2.27)$$

where  $\delta_{\chi\phi} \equiv \delta\chi/\dot{\chi} - \delta\phi/\dot{\phi} = \dot{\sigma}/(\dot{\phi}\dot{\chi})\delta s$ . Neglecting the contribution from the  $\delta\dot{s}$  term, the isocurvature perturbation can be written in terms of the entropy field perturbation,  $\delta s$ , as

$$S_{\chi\phi} = T_{\chi\phi} \delta s, \quad \text{with} \quad T_{\chi\phi} \simeq -3 \frac{\sqrt{4\pi}}{M_p} \frac{\sqrt{\epsilon_t}}{(\pm\sqrt{\epsilon_\phi})(\pm\sqrt{\epsilon_\chi})}. \quad (2.28)$$

We note that when the slow-roll conditions are violated, the  $\delta\dot{s}$  term may provide a contribution to the isocurvature perturbation that is not captured by eq. (2.28) which can induce small differences when compared with the definition (2.27).

Making use of eq. (2.28), the power spectrum of the isocurvature perturbation at the end of inflation is found to be

$$\mathcal{P}_S = \left( \frac{H_k}{2\pi} \right)^2 T_{\chi\phi}^2 |g^2(t_f)| \simeq \frac{9}{\pi} \left( \frac{H_k}{M_p} \right)^2 \frac{\epsilon_t(t_f)}{\epsilon_\phi(t_f)\epsilon_\chi(t_f)} |g^2(t_f)|. \quad (2.29)$$

The cross-spectrum between  $Q_\sigma$  and  $\delta s$  is estimated as  $P_{Q\delta s} = (H_k/2\pi)^2 g(t)P(t)$  from eq. (2.15). Then we find the cross-spectrum between  $\mathcal{R}$  and  $S$  as

$$\mathcal{P}_C = \left( \frac{H_k}{2\pi} \right)^2 \frac{H(t_f)}{\dot{\sigma}(t_f)} T_{\chi\phi} g(t_f) P(t_f) \simeq -\frac{6}{\pi} \left( \frac{\dot{\theta}}{H} \right)_k \left( \frac{H_k}{M_p} \right)^2 \frac{e^{\zeta_k N_k} - 1}{\zeta_k} \frac{|g^2(t_f)|}{(\pm\sqrt{\epsilon_\phi(t_f)})(\pm\sqrt{\epsilon_\chi(t_f)})}. \quad (2.30)$$

The spectral indices for the power-spectrum,  $\mathcal{P}$ , is defined by

$$n - 1 \equiv \frac{d \ln \mathcal{P}}{d \ln k} = (1 + \epsilon_t) \frac{d \ln \mathcal{P}}{d \ln a} \Big|_{k=aH}. \quad (2.31)$$

Therefore the spectral indices for  $\mathcal{P}_{\mathcal{R}}$ ,  $\mathcal{P}_S$ , and  $\mathcal{P}_C$  read [31]

$$n_{\mathcal{R}} - 1 = -6\epsilon_t + 2 \frac{\epsilon_\phi \eta_{\phi\phi} + \epsilon_\chi \eta_{\chi\chi}}{\epsilon_t} + 4 \frac{(\pm\sqrt{\epsilon_\phi})(\pm\sqrt{\epsilon_\chi})}{\epsilon_t} \eta_{\phi\chi} - \frac{8|f^2(t_f)|}{|f^2(t_f)| + |P^2(t_f)|} \left( \frac{\dot{\theta}}{H} \right)_k^2 \frac{e^{-\zeta_k N_k}}{\zeta_k} (1 - e^{-\zeta_k N_k}), \quad (2.32)$$

$$n_S - 1 = -2\epsilon_t + 2 \frac{\epsilon_\phi \eta_{\chi\chi} + \epsilon_\chi \eta_{\phi\phi}}{\epsilon_t} - 4 \frac{(\pm\sqrt{\epsilon_\phi})(\pm\sqrt{\epsilon_\chi})}{\epsilon_t} \eta_{\phi\chi}, \quad (2.33)$$

$$n_C - 1 = -2\epsilon_t + 2 \frac{\epsilon_\phi \eta_{\chi\chi} + \epsilon_\chi \eta_{\phi\phi}}{\epsilon_t} - 4 \frac{(\pm\sqrt{\epsilon_\phi})(\pm\sqrt{\epsilon_\chi})}{\epsilon_t} \eta_{\phi\chi} - \frac{\zeta_k e^{\zeta_k N_k}}{e^{\zeta_k N_k} - 1}, \quad (2.34)$$

where the slow-roll parameters are evaluated at horizon crossing. The spectrum  $P_T$  and the spectral index  $n_T$  of tensor perturbations are calculated by analyzing the equation of massless gravitational fields [3]:

$$P_T = \left( \frac{4}{\sqrt{\pi}} \frac{H_k}{M_p} \right)^2, \quad n_T = -\frac{8\pi}{M_p^2} \left( \frac{\dot{\sigma}}{H} \right)_k^2. \quad (2.35)$$

We introduce two ratios  $r_C$  and  $r_T$ , which are defined as

$$r_C \equiv \frac{P_C}{\sqrt{P_{\mathcal{R}} P_S}}, \quad (2.36)$$

and

$$r_T \equiv \frac{P_T}{16P_{\mathcal{R}}}. \quad (2.37)$$

From eqs. (2.26), (2.29) and (2.30) we find that the correlation ratio  $r_C$  can be expressed as

$$r_C = \frac{x}{\sqrt{1+x^2}}, \quad \text{with} \quad x = \frac{P(t_f)}{f(t_f)}. \quad (2.38)$$

Therefore  $r_C^2$  lies in the range  $0 \leq r_C^2 \leq 1$ . Note that the relation (2.38) is obtained without assuming that the adiabatic/entropy masses and  $\dot{\theta}/H$  are constant after horizon crossing. Namely, the equality  $\simeq$  in eqs. (2.26), (2.29) and (2.30) is not used when we derive eq. (2.38). If the slow-roll solutions (2.21) are employed, we have

$$x \simeq 2 \left( \frac{\dot{\theta}}{H} \right)_k \frac{1 - e^{-\zeta_k N_k}}{\zeta_k}. \quad (2.39)$$

The behaviour of the term  $\dot{\theta}/H$  is most important when we analyze the correlation between adiabatic and isocurvature perturbations. In eq. (2.39) the ‘‘frozen’’ value of  $\dot{\theta}/H$  is used at horizon crossing. However, since the assumption of constant  $\dot{\theta}/H$  is not generally valid during double inflation, the slow-roll result (2.39) leads to some errors in estimating  $r_C$  at the end of double inflation. When  $\dot{\theta}/H$  varies significantly, we have to integrate this term from first horizon crossing to the end of inflation rather than use the ‘‘frozen’’ value at horizon crossing. Note that if  $\dot{\theta}/H$  is vanishingly small during the *both* phases of inflation the correlation vanishes ( $r_C = 0$ ).

The tensor to scalar ratio  $r_T$  can be evaluated without using the slow-roll equality in eqs. (2.26) and (2.35), as

$$r_T = \frac{4\pi}{M_p^2} \left( \frac{\dot{\sigma}(t_f)}{H(t_f)} \right)^2 \frac{1}{|f^2(t_f)| + |P^2(t_f)|} = \frac{4\pi}{M_p^2} \left( \frac{\dot{\sigma}}{H} \right)_k^2 \frac{1}{1+x^2}. \quad (2.40)$$

Here we used the fact that  $(H/\dot{\sigma})f$  is conserved after horizon crossing, i.e.,  $(H/\dot{\sigma})_k = (H(t_f)/\dot{\sigma}(t_f))f(t_f)$  [see eq. (2.25) with  $k \ll aH$  and  $\delta s = 0$ ]. Making use of eqs. (2.35), (2.38) and (2.40) we get the consistency relation

$$r_T = -\frac{n_T}{2} (1 - r_C^2). \quad (2.41)$$

This indicates that the correlation between adiabatic and isocurvature perturbations leads to the modification of the consistency relation in the single field case ( $r_T = -n_T/2$ ).

In deriving eq. (2.41), we did not exploit the assumption that the adiabatic/entropy mass and  $\dot{\theta}/H$  are constant after horizon crossing. Then this consistency relation should be valid as long as the slow-roll conditions are satisfied at *horizon crossing*, in which case the uncorrelated solutions for  $Q_\sigma$  and  $\delta s$  can be used at  $k = aH$  [34]<sup>3</sup>. In the context of double inflation there are some cases where the slow-roll conditions can be violated at horizon crossing, implying that the consistency relation (2.41) does not hold automatically when applied to realistic double inflation models.

The authors in ref. [31] obtained the following second consistency relation from the slow-roll results (2.32)-(2.34) together with (2.35) and (2.40), as

$$(n_C - n_S) r_T = -\frac{n_T}{4} (2n_C - n_{\mathcal{R}} - n_S) . \quad (2.42)$$

Note that the constancy of the adiabatic/entropy mass and  $\dot{\theta}/H$  is assumed in deriving this relation. Therefore it is likely that the second consistency relation (2.42) is more strongly affected by the violation of the slow-roll conditions compared to the first consistency relation (2.41).

While the slow-roll results which include the quantities  $n_{\mathcal{R}}$ ,  $n_S$ , and  $n_C$  can exhibit strong deviation from the numerical results, the spectral index  $n_T$  of the gravitational wave is well described by eq. (2.35) even in the context of double inflation. Therefore provided that the correlation is small at horizon crossing, the first consistency relation (2.41) is expected to be reliable as long as we use  $x$  in eq. (2.38) instead of the slow-roll result in eq. (2.39).

In the following section we shall compare the above formula with full numerical simulations for concrete models of double inflation. We will provide a detailed analysis of the spectra of perturbations and the validity of the consistency relations derived from the above analysis. We will also discuss the parameter ranges where the correlation of adiabatic and isocurvature perturbations is strong.

### III. DOUBLE INFLATION WITH TWO MASSIVE SCALAR FIELDS

Let us first consider a simple model where massive scalar fields,  $\phi$  and  $\chi$ , are coupled through an interaction term  $\frac{1}{2}g^2\phi^2\chi^2$ :

$$V(\phi, \chi) = \frac{1}{2}m_\phi^2\phi^2 + \frac{1}{2}m_\chi^2\chi^2 + \frac{1}{2}g^2\phi^2\chi^2 . \quad (3.1)$$

There are three parameters associated with this potential:  $m_\phi$ ,  $m_\chi$  and  $g$ . Then there are four free parameters associated with the initial conditions of the fields:  $\phi_i$ ,  $\chi_i$ ,  $\dot{\phi}_i$  and  $\dot{\chi}_i$ . Making use of the slow roll approximation,  $\dot{\phi} = -V_\phi/3H$  and  $\dot{\chi} = -V_\chi/3H$  with  $H^2 = (8\pi/3M_p^2)V$  in eqs. (2.1) and (2.2), the initial conditions of  $\dot{\phi}$  and  $\dot{\chi}$  are determined by  $\phi_i$  and  $\chi_i$ <sup>4</sup>. This assumption cuts down the number of free parameters to two,  $\phi_i$  and  $\chi_i$ . Therefore we have five free parameters ( $m_\phi$ ,  $m_\chi$ ,  $g$ ,  $\phi_i$  and  $\chi_i$ ) for the model (3.1). Once these parameters are given, the evolution of the background is determined, with the number of e-folds,  $N = -\ln(a/a_f)$ , with  $a_f$  being the value of the scale factor at the end of inflation [13]. We shall introduce the number of e-folds,  $N_H$ , which corresponds to the value of  $N$  when the scale corresponding to our Hubble radius today crossed out the Hubble radius during inflation. Hereafter we set it to be

$$N_H = 60 , \quad (3.2)$$

in order to make definite calculations.

---

<sup>3</sup>Note that the decaying mode for  $\mathcal{R}$  can be important in some non slow-roll inflationary scenarios [54,55]. In this case the second derivatives of eqs. (2.9) and (2.14) are not necessarily small and the first term in the rhs of eq. (2.15) is not negligible. Then we need to add the decaying mode solutions to eq. (2.15). The consistency relation (2.41) does not cover this case, although the enhancement of the decaying mode occurs only in some restricted situations [54,55].

<sup>4</sup>Clearly assuming slow-roll to set the initial conditions is not generally valid. Not assuming this will lead to extra transient violations of the slow-roll conditions but if inflation is successfully initiated, the fields should settle to their slow-roll values quickly. At any rate our interest is in correlations and violations of the slow-roll approximation in a minimal sense. Inverting CMB and LSS data to give information about the potential and initial conditions will have to deal with this possibility in general however.

### A. Non-interacting fields: $g = 0$

In the case where the fields are non-interacting ( $g = 0$ ), the slow-roll approximation in eqs. (2.1) and (2.2) gives the relation  $\phi^2 + \chi^2 = 4N/\kappa^2$ . The fields lie on a circle of radius  $2\sqrt{N}/\kappa$ . Therefore it is useful to write  $\phi$  and  $\chi$  in parametric form [13]:

$$\phi = \frac{2\sqrt{N}}{\kappa} \cos \alpha, \quad \chi = \frac{2\sqrt{N}}{\kappa} \sin \alpha. \quad (3.3)$$

This means that the evolution of two scalar fields is characterised by  $N$  and the scalar field position angle,  $\alpha$ , satisfying the relation  $\tan \alpha = \chi/\phi$ . The field velocity angle,  $\theta$ , defined by eq. (2.7) is related to  $\alpha$  by

$$\tan \theta \simeq -\frac{2m_\chi^2\sqrt{N}}{3H\kappa\dot{\sigma}} \tan \alpha. \quad (3.4)$$

Making use of the relation (3.3), we find that the number of e-folds can be expressed as [13]

$$N = N_0 \frac{(\sin \alpha)^{2/(R^2-1)}}{(\cos \alpha)^{2R^2/(R^2-1)}}, \quad (3.5)$$

where

$$R \equiv m_\chi/m_\phi. \quad (3.6)$$

Note that the integration constant,  $N_0$ , roughly corresponds to the number of e-folds during the second stage of inflation driven by the light scalar field. Hereafter we shall concentrate on the case where the field  $\chi$  is heavier than  $\phi$ , i.e.,  $R > 1$ .

In order to know the evolution of the background we need to determine four parameters:  $m_\phi$ ,  $R$ ,  $N_0$ , and  $\alpha$ . When the total number of e-folds is fixed at around  $N_H$ , the model parameters are reduced to three ( $m_\phi$ ,  $R$  and  $N_0$ ). Whether inflation is dominated by the heavy or light fields when the scale of cosmological relevance crosses the Hubble radius depends on the value of  $N_0$  relative to  $N_H = 60$ .

Adiabatic perturbations for modes larger than the Hubble radius during the radiation dominant era can be matched with the curvature perturbation at the end of inflation, which are given by [24,8]

$$\mathcal{R} \simeq -\frac{\kappa^2 H(t_*)}{2\sqrt{2}k^3} [\phi(t_*)e_\phi(\mathbf{k}) + \chi(t_*)e_\chi(\mathbf{k})] = -\frac{\kappa H(t_*)\sqrt{N}}{\sqrt{2}k^3} [\cos \alpha_* e_\phi(\mathbf{k}) + \sin \alpha_* e_\chi(\mathbf{k})], \quad (3.7)$$

where  $\alpha_*$  is the value of  $\alpha$  at the horizon crossing. Assuming that the field  $\phi$  decays into ordinary matter (baryons, photons, neutrinos) and  $\chi$  into cold dark matter, super-Hubble isocurvature perturbations during the radiation dominant era is expressed as [24,8]

$$S \simeq \frac{H(t_*)}{\sqrt{2}k^3} \left[ R^2 \frac{e_\phi(\mathbf{k})}{\phi(t_*)} - \frac{e_\chi(\mathbf{k})}{\chi(t_*)} \right] = \frac{\kappa H(t_*)}{2\sqrt{N}\sqrt{2}k^3} \left[ R^2 \frac{e_\phi(\mathbf{k})}{\cos \alpha_*} - \frac{e_\chi(\mathbf{k})}{\sin \alpha_*} \right]. \quad (3.8)$$

The expression (3.7) indicates that for the adiabatic perturbation the heavy field  $\chi$  dominates for  $\tan \alpha_* > 1$ , while the light field  $\phi$  dominates for  $\tan \alpha_* < 1$ . From eq. (3.8) we find that for the isocurvature perturbation the heavy field  $\chi$  dominates for  $\tan \alpha_* < 1/R^2$ , while the light field  $\phi$  dominates for  $\tan \alpha_* > 1/R^2$ .

Let us estimate the correlation  $r_C$  that is derived from the slow-roll analysis, see eq. (2.38) with (2.39). This is not actually completely valid as we pointed out in the previous section, but useful to make rough estimation for the correlation. We will check, of course, the validity of the analytic estimates by numerical simulations. By a simple calculation we find that  $x$  defined in eq. (2.39) is given by

$$x = \frac{R^2(R^2-1)\tan \alpha_*(1+\tan^2 \alpha_*)}{(1+R^2\tan^2 \alpha_*)(1+R^4\tan^2 \alpha_*)} \frac{1-e^{-\zeta_k N_k}}{\zeta_k N_k}. \quad (3.9)$$

If the condition,  $|\zeta_k|N_k \ll 1$ , is satisfied, this reduces to

$$x = \frac{R^2(R^2-1)\tan \alpha_*(1+\tan^2 \alpha_*)}{(1+R^2\tan^2 \alpha_*)(1+R^4\tan^2 \alpha_*)}. \quad (3.10)$$

Note that when  $|\zeta_k|N_k \gtrsim 1$  one has  $|(1 - e^{-\zeta_k N_k})/(\zeta_k N_k)| \simeq 1/|(\zeta_k N_k)| \lesssim 1$ . Therefore the value of  $x$  is smaller than in the case of (3.10). Eq. (2.38) implies that the correlation  $r_C$  vanishes for  $x = 0$  and gets larger for increasing  $x$ . In particular when  $x$  is larger than of order unity, the correlation is strong ( $r_C$  is close to unity). From eq. (3.9) we find that there is no correlation if the masses of the scalar fields are equal ( $R = 1$ ). We can also make consistency check by using eq. (3.9) or (3.10). When the masses of the scalar fields differ significantly ( $R \rightarrow 0$  or  $R \rightarrow \infty$ ), the correlation is also vanishingly small for fixed  $\tan \alpha_*$ .

In order to discuss the correlation precisely, it is useful to classify model parameters into three cases [24]: (a)  $\tan \alpha_* \gg 1$ , (b)  $\tan \alpha_* \ll 1/R^2$  and (c)  $1/R^2 < \tan \alpha_* < 1$ . Hereafter we shall analyze the strength of the correlation as well as the power spectra and consistency relations, and check the validity of the slow-roll analysis.

**(a)  $\tan \alpha_* \gg 1$**

In this case the field  $\chi$  is the main source for adiabatic perturbations, while isocurvature perturbations are dominated by the field  $\phi$ . Therefore both perturbations are regarded as almost independent ones, and the correlation is weak (see Fig. 1). In fact when  $\tan \alpha_* \gg 1$  eq. (3.10) yields

$$x \simeq \frac{R^2 - 1}{R^4} \frac{1}{\tan^2 \alpha_*}. \quad (3.11)$$

Therefore the correlation  $r_C$  decreases with increasing  $\tan \alpha_*$  and one has  $r_C \rightarrow 0$  for  $\tan \alpha_* \rightarrow \infty$ . This decreasing rate is more significant for larger  $R$  as can be seen from eq. (3.11) and Fig. 2.

The amplitude of isocurvature perturbations is not typically larger than that of adiabatic perturbations unless  $\alpha_*$  is so much close to  $\pi/2$ , as shown in Fig. 3.<sup>5</sup> Since the correlation term in eq. (2.32) is neglected and  $\epsilon_\phi \ll \epsilon_\chi$  for  $\tan \alpha_* \gg 1$ , one has a spectral index of the curvature perturbation that is approximately the same as the single field case:

$$n_{\mathcal{R}} - 1 \simeq -6\epsilon_\chi + 2\eta_{\chi\chi} = -\frac{1}{\pi} \left( \frac{M_p}{\chi} \right)^2. \quad (3.12)$$

This is a slowly red-tilted spectrum as found in Fig. 3. In the right panel of Fig. 3 we also plot the ratio  $r_T$  defined by eq. (2.37) and its value obtained by two consistency relations (2.41) and (2.42). Except for some discontinuous behaviour which is accompanied with numerics<sup>6</sup>, consistency relations show fairly good agreement with the value of the original definition of  $r_T$ . In this case since  $r_C$  is much less than unity in this case the consistency relation (2.41) is practically no different from that of the single field case,  $r_T = -n_T/2$ . Namely it is almost the same as the single field inflation driven by only one scalar field. Therefore the assumption that  $\mu_Q^2/(3H^2)$ ,  $\mu_s^2/(3H^2)$  and  $\dot{\theta}/H$  do not vary too much during inflation can be justified in this case, so not giving strong deviation in the consistency relations.

**(b)  $\tan \alpha_* \ll 1/R^2$**

In this case the field  $\phi$  is the main source for adiabatic perturbations, while isocurvature perturbations are dominated by the field  $\chi$ . From eq. (3.10) one has

$$x \simeq R^4 \tan \alpha_*, \quad (3.13)$$

for  $R^2 \tan \alpha_* \ll 1$ . Therefore adiabatic and isocurvature perturbations are almost independent from each other for smaller  $\tan \alpha_*$ , which can be confirmed in Fig. 1. In Fig. 2 we find that the prediction (3.10) overestimates the correlation ratio  $r_C$  when  $\tan \alpha_*$  is small, while eq. (3.9) shows fairly good agreement with numerical results. This implies that  $|\zeta_k|N_k$  could be larger than unity, in which case the  $(1 - e^{-\zeta_k N_k})/(\zeta_k N_k)$  term can not be neglected in eq. (3.9).

When  $\tan \alpha_* \ll 1/R^2$  the amplitude of isocurvature perturbations are larger than that of adiabatic ones as predicted by eqs. (3.7) and (3.8) [see Fig. 3]. The spectrum of curvature perturbations is hardly affected by isocurvature

<sup>5</sup>Note, however, that the amplitude of isocurvature perturbations can be high if  $\alpha_*$  is very close to  $\pi/2$ .

<sup>6</sup>We evaluated the spectral indices numerically using the definition,  $n = 1 + \Delta(\ln P)/\Delta(\ln k)$ , which leads to some numerical errors and some spikiness in some of the figures.

perturbations because the correlation is small ( $r_C \ll 1$ ). Therefore the consistency relation in the single-field case should not be significantly modified in this case.

In fact, from Fig. 3 we find that the first consistency relation (2.41) shows good agreement with the original definition of  $r_T$ , while the second one (2.42) is not so good. Indeed we should expect deviations from the predictions of the second consistency relation around the end of inflation because the masses of the adiabatic/entropy fields and  $\dot{\theta}/H$  are not constant in this case. Even in the case (a) the discrepancy in the second consistency relation is a bit larger than in the case of the first one.

$$(c) \quad 1/R^2 \leq \tan \alpha_* \leq 1$$

In this case both adiabatic and isocurvature perturbations are sourced by the light field  $\phi$ , but the effect of the heavy field  $\chi$  is also important. From eq. (3.11) we find

$$x = \frac{(R^2 - 1)(R^4 + 1)}{2R^2(R^2 + 1)}, \quad \text{for} \quad \tan \alpha_* = \frac{1}{R^2}, \quad (3.14)$$

and

$$x = \frac{2R^2(R^2 - 1)}{(R^2 + 1)(R^4 + 1)}, \quad \text{for} \quad \tan \alpha_* = 1. \quad (3.15)$$

Therefore when  $\tan \alpha_* = 1/R^2$  and  $R$  is not too close to unity,  $x$  is typically larger than unity (for example one has  $x > 1.275$  for  $R > 2$ ). In this case the correlation ratio  $r_C$  is close to 1. The range of this high correlation gets wider for larger  $R$  as found in Fig. 2. When  $\tan \alpha_* \simeq 1$ ,  $x$  is at a maximum  $x_{\max} \simeq 0.3$  for  $R \simeq 1.7$ , with the correlation ratio ranges  $r_C \leq 0.28$  in this case. As  $R$  is increased, the maximum correlation becomes smaller, as is seen in Fig. 2.

Note that we need to include the correction term  $(1 - e^{-\zeta_k N_k})/(\zeta_k N_k)$  in eq. (3.9) to accurately estimate the strength of the correlation. Fig. 2 clearly indicates that the correlation is strong around  $1/R^2 \leq \tan \alpha_* \leq 1$ . In this case the correlation term  $r_C^2$  is very important in the consistency relation, (2.41), because  $r_C$  will be close to unity. Fig. 2 seems to show good agreement between the predicted value of  $r_C$  and value obtained numerically around  $1/R^2 \leq \tan \alpha_* \leq 1$ .

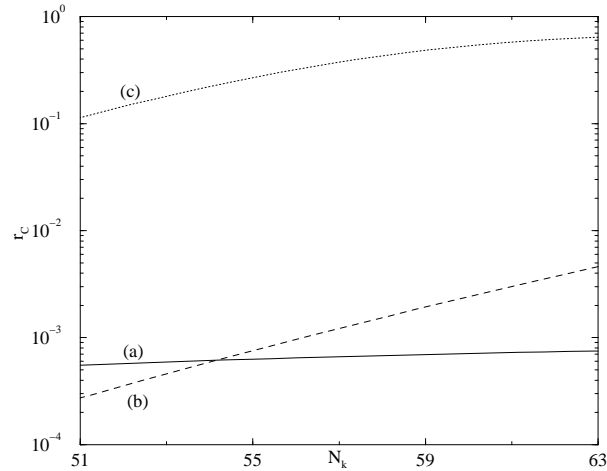


FIG. 1: Correlation spectra  $r_C$  for three different cases with  $R = 5$ ,  $m_\phi = 2.0 \times 10^{-7} M_p$  and  $g = 0$ . Each case corresponds to (a)  $\tan \alpha = 32.0 \gg 1$ , (b)  $\tan \alpha = 3.13 \times 10^{-4} \ll R^{-2}$ , and (c)  $R^{-2} < \tan \alpha = 0.16 < 1$ , on the scale  $N_k = 65$ . The case (c) shows strong correlations, while the cases (a) and (b) are not.

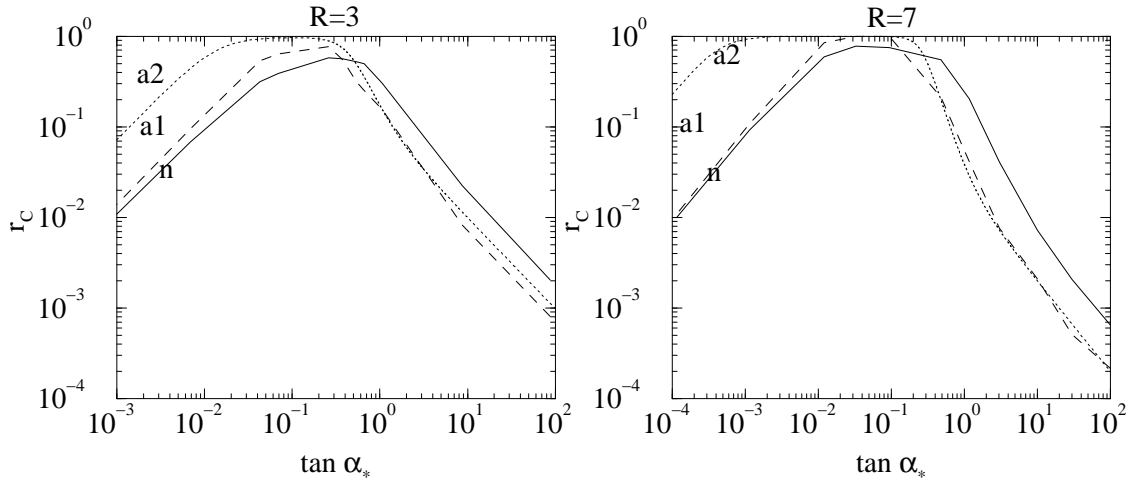


FIG. 2: The correlation  $r_C$  as a function of  $\tan \alpha_*$  for  $R = 3$  and  $R = 7$  with  $m_\phi = 2.0 \times 10^{-7} M_p$  and  $g = 0$  on the scale corresponding to  $N_k = 60$ . The solid curve corresponds to the numerical result, while dashed (“a1”) and dotted (“a2”) curves correspond to the results using eqs. (3.9) and (3.10), respectively.

However, the figure has a logarithmic scale for  $r_C$  and in the consistency relation (2.41) it is  $r_C^2$  that is important. As found from Fig. 2 analytic estimates by slow-roll approximations typically give larger values of  $r_C$  around the region where the correlation is strong. When  $r_C$  is close to unity, this difference can affect the consistency relation (2.41). In Fig. 4 we plot the evolution of  $\mu_Q^2/(3H^2)$ ,  $\mu_s^2/(3H^2)$  and  $\dot{\theta}/H$  for  $R = 5$ ,  $m_\chi = 1 \times 10^{-6} M_p$  and  $g = 0$  with initial conditions  $\chi = 3M_p$  and  $\phi = 1.5M_p$ . The heavy field  $\chi$  leads to the first phase of inflation until  $\tau \equiv 10^{-6} M_p t \simeq 20$ , which is followed by the second stage of inflation driven by  $\phi$ . All of  $\mu_Q^2/(3H^2)$ ,  $\mu_s^2/(3H^2)$  and  $\dot{\theta}/H$  exhibit rapid increase around the end of the first stage of inflation due to the breakdown of the slow-roll conditions for  $\chi$ . For example,  $\mu_s^2/(3H^2)$  continues to grow by the end of the second stage of inflation, whose growth is about  $5 \times 10^4$  times compared to its initial value.

In this case the assumption of the constancy of the mass terms is no longer justified in eqs. (2.17) and (2.21), thereby leading to errors in the correlation  $r_C$  if we use the estimation in eq. (2.39). In addition, the peak value of  $\dot{\theta}/H$  typically provides a larger contribution than its value at horizon crossing in eq. (2.39). Therefore we need to evaluate the values of  $x$  and  $r_C$  numerically in order to estimate the correlation accurately.

In the case where the correlation is strong at horizon crossing, we expect to find deviations even from the predictions of the first consistency relation. In fact the numerical result in Fig. 3 (c) does not show good agreement with the slow-roll results. This case corresponds to the one where the slow-roll conditions are violated at horizon crossing, thereby showing some deviations from the result (2.41). We have numerically checked that the first consistency relation holds well as long as the slow-roll conditions are satisfied at horizon crossing, which agrees with the claim by Wands *et al* [34]. The second consistency relation is more strongly affected by the violation of the slow-roll conditions during double inflation, especially when the correlation is strong. The slow-roll analysis shows some limitations to correctly estimate three spectral indices  $n_{\mathcal{R}}$ ,  $n_S$ , and  $n_C$ . Numerical analysis is required as well in order to fully understand the strength of the correlation and the final power spectra of adiabatic and isocurvature perturbations.

In Fig. 1 we find that the correlation is high around  $N_k \gtrsim 60$ , and decreases toward smaller scales. This corresponds to the “light” inflationary phase with  $\theta \lesssim 1/R$  where the perturbations are mainly sourced by the field  $\phi$  around  $N_k \simeq 60$ . In this case the correlation gets weaker toward smaller scales due to the decrease of  $\dot{\theta}$ . If the scale  $N_k = 60$  corresponds to the “heavy” inflationary phase with  $\alpha \gtrsim 1/R$ , the correlation  $r_C$  is nearly constant as shown in ref. [24]. This means that  $\alpha$  varies slowly during the heavy field inflation, which makes  $\dot{\theta}$  unsuppressed. The slow variation of  $r_C$  can be actually found in the case (a) of Fig. 1. Note that if we choose the value of  $\alpha$  not much greater than  $1/R$  the correlation can be higher as claimed in ref. [24].

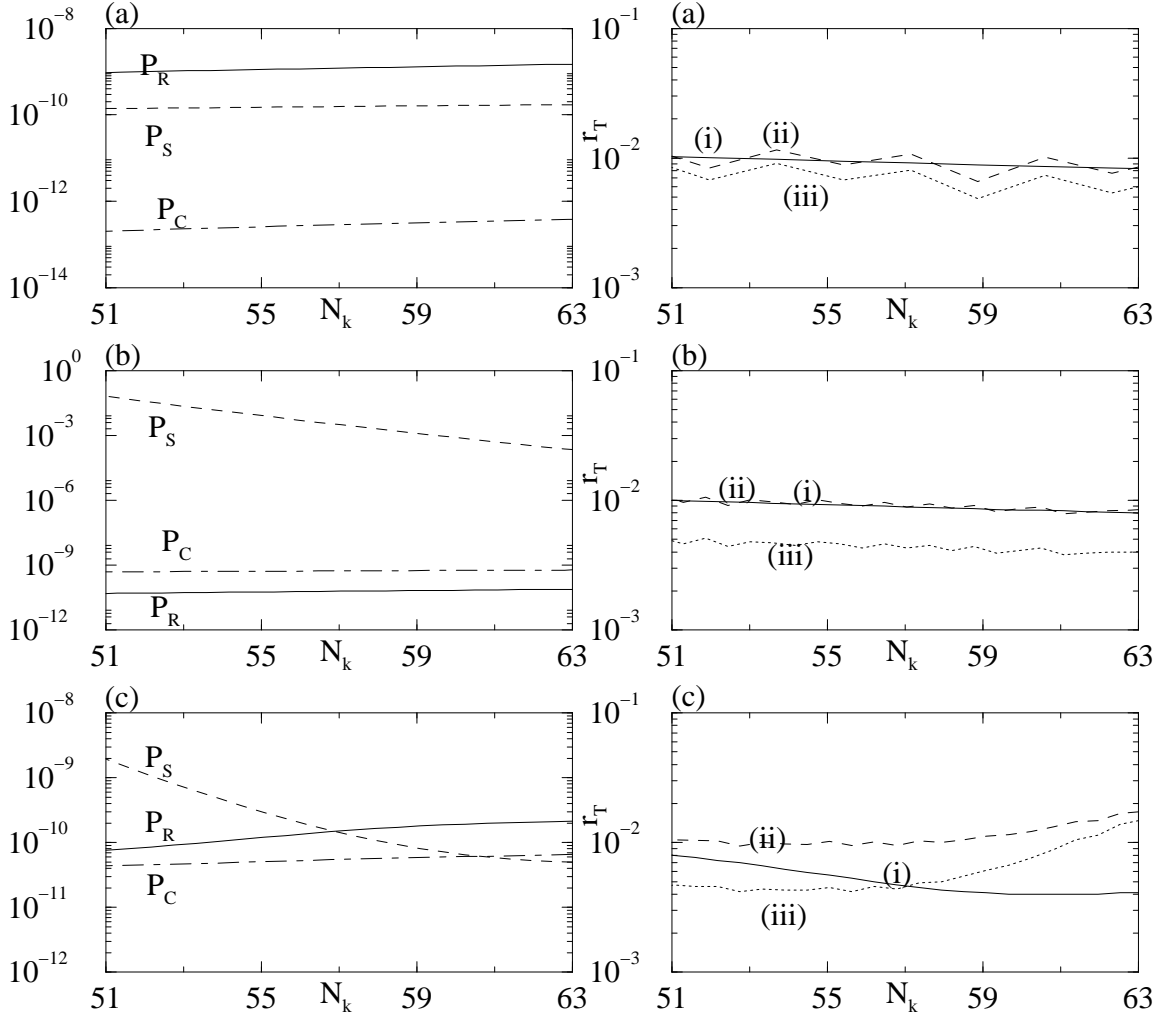


FIG. 3: The power spectra  $P_R$ ,  $P_S$  and  $P_C$  (left panel) with  $R = 5$ ,  $m_\phi = 2.0 \times 10^{-7} M_p$  and  $g = 0$ . The curves correspond to the cases (a)  $\tan \alpha = 32.0 \gg 1$  (heavy-field dominated), (b)  $\tan \alpha = 3.13 \times 10^{-4} \ll R^{-2}$  (light-field dominated), and (c)  $R^{-2} < \tan \alpha = 0.16 < 1$ , on the scale corresponding to  $N_k = 65$  (double inflation). The right panel shows the ratio  $r_T$  that is derived by using eq. (2.36), and the two consistency relations eq. (2.41) and (2.42), which are denoted by (i), (ii), (iii), respectively. Note that while the  $r_T$  calculated numerically, (i), typically agreed with (ii), it often differs from (iii) due to time-dependent adiabatic/entropy masses or  $\theta \neq 0$ ; see e.g., Fig. 4.

Two important quantities to determine the strength of the correlation are  $R$  and  $\tan \alpha_*$  around  $N_H \simeq 60$  as seen from eq. (3.9). The e-folding of the second stage of inflation,  $N_0$ , determines whether inflation is dominated by a heavy or light scalar field around  $N_H \simeq 60$  and also the strength of the correlation on smaller scales. Either of the scalar field masses,  $m_\phi$  or  $m_\chi$ , can be determined by the COBE normalization. The relative ratio  $R = m_\chi/m_\phi$  is important when we discuss the correlation,  $r_C$ . The correlation is strong around  $1/R^2 \leq \tan \alpha_* \leq 1$ , whose lower bound is also determined by  $R$ . If the precise observations in the future reveals the strength of the correlation around  $50 \lesssim N_k \lesssim 63$ , we will be able to constrain on two masses  $m_\phi$  and  $m_\chi$  (alternatively  $R$  and  $m_\phi$ ) together with the values of  $\tan \alpha_*$  and  $N_0$ .

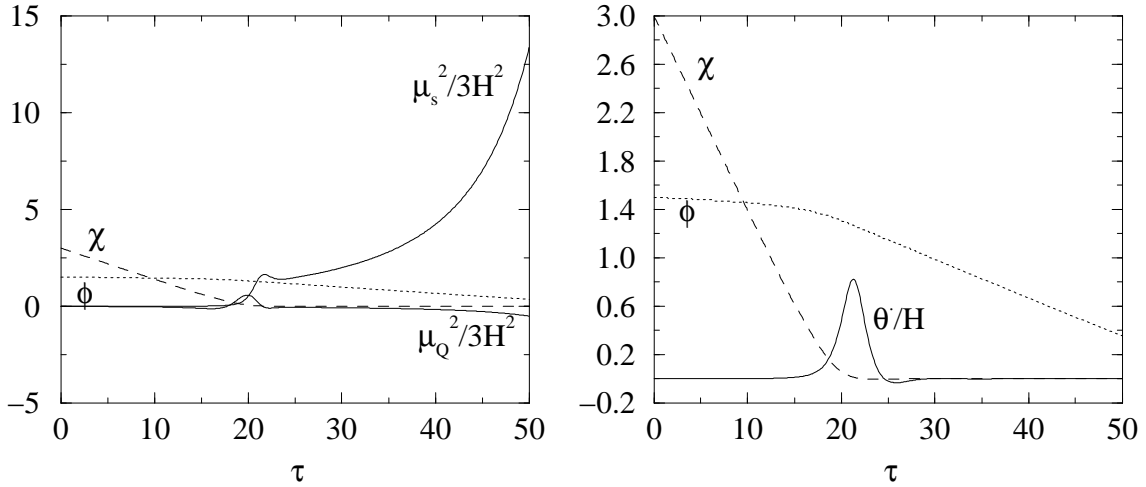


FIG. 4: The evolution of  $\mu_Q^2/(3H^2)$  and  $\mu_s^2/(3H^2)$  (on the left) and  $\dot{\theta}/H$  (on the right) with  $R = 5$ ,  $m_\chi = 1 \times 10^{-6} M_p$  and  $g = 0$ . The initial conditions are chosen to be  $\chi = 3M_p$  and  $\phi = 1.5M_p$ . When the heavy field drops to the potential valley, a second phase of inflation begins, which is accompanied by the increase of  $\mu_Q^2/(3H^2)$ ,  $\mu_s^2/(3H^2)$  and  $\dot{\theta}/H$ . The term  $\mu_s^2/(3H^2)$  exhibits the growth by a factor of  $5 \times 10^4$  by the end of inflation compared to its initial value.  $\dot{\theta}/H$  grows from the initial value  $1.44 \times 10^{-3}$  to its peak value  $\dot{\theta}/H = 0.8$  around the end of the first stage of inflation.

### B. The interacting case: $g \neq 0$

Let us next consider the case where the coupling  $g$  is taken into account. It was suggested by Linde and Mukhanov [18] that inclusion of the coupling  $g$  can lead to the blue spectrum of isocurvature perturbations. Here we shall make detailed analysis about the correlation of adiabatic and isocurvature perturbations.

Let us first estimate the spectrum of isocurvature perturbations using the analytic estimates of Sec. II. Although it has some errors due to the breakdown of slow-roll approximations, it is still useful to make rough estimates for the power spectrum. The spectral index in eq. (2.33) is estimated as

$$n_S - 1 = -2\epsilon_t + \frac{2\mu_s^2}{3H^2}, \quad (3.16)$$

Therefore it is important to consider the mass of the entropy field perturbation,  $\mu_s$ , relative to the Hubble rate,  $H$ . Note that the term  $-2\epsilon_t$  in the rhs of eq. (3.16) provides the slowly red-tilted spectrum. If the mass square  $\mu_s^2$  is larger than of order  $H^2$ , isocurvature perturbations are blue-tilted with  $n_S > 1$ . Making use of the slow-roll result (2.18), we find

$$\frac{2\mu_s^2}{3H^2} = \frac{4(m_\chi^2 + g^2\phi^2)(m_\phi^2 + g^2\chi^2)(m_\phi^2\phi^2 + m_\chi^2\chi^2 - 2g^2\phi^2\chi^2)}{\kappa^2(m_\phi^2\phi^2 + m_\chi^2\chi^2 + g^2\phi^2\chi^2) \left\{ (m_\phi^2 + g^2\chi^2)^2\phi^2 + (m_\chi^2 + g^2\phi^2)^2\chi^2 \right\}}. \quad (3.17)$$

Let us first consider the case where  $\mu_s^2$  is positive during the whole stage of double inflation, which corresponds to the condition,  $m_\phi^2\phi^2 + m_\chi^2\chi^2 > 2g^2\phi^2\chi^2$ . When the heavy field  $\chi$  rolls down to the valley  $\chi = 0$  at the first stage of inflation, we have  $\mu_s^2 \simeq m_\chi^2 + g^2\phi^2$  and  $3H^2 \simeq 4\pi m_\phi^2\phi^2/M_p^2$ . Then the mass square of  $\delta s$  is given by

$$\mu_s^2 \simeq m_\chi^2 + \beta H^2, \quad \text{with} \quad \beta = \frac{3g^2}{4\pi} \left( \frac{M_p}{m_\phi} \right)^2. \quad (3.18)$$

Note that in this case the entropy field perturbation  $\delta s$  is almost the same as the heavy field perturbation  $\delta\chi$ . If  $\chi$  is quickly suppressed, we only need to consider  $\delta\chi$ , as in ref. [18], in order to discuss the spectrum of isocurvature perturbations. When  $\beta H^2$  is larger than  $m_\chi^2$  during double inflation, we have  $\mu_s^2 \simeq \beta H^2$  and

$$n_S - 1 \simeq -2\epsilon_t + \frac{2}{3}\beta. \quad (3.19)$$

When  $\beta$  is much larger than unity, this yields the blue-tilted spectrum,  $n_S > 1$ .<sup>7</sup> Making use of this scenario, it is possible to obtain isocurvature perturbations that tend to grow toward smaller scales while adiabatic perturbations remain small on present horizon scales [18]. If  $\mu_s^2 \gg H^2$ , then  $\chi$  rolls down very rapidly to the local minimum of the potential valley ( $\chi \rightarrow 0$ ), and  $\dot{\theta}$  in eq. (2.30) exponentially decreases on smaller scales. In this case the correlation between adiabatic and isocurvature perturbations tends to be very weak except for the scales where  $\chi$  is not very small compared to  $\phi$ . When  $\dot{\theta}$  is negligible, the spectrum of curvature perturbations is practically no different from the single field result,  $n_{\mathcal{R}} - 1 = -6\epsilon_\phi + 2\eta_{\phi\phi}$  [see eq. (2.32)]. In this case adiabatic perturbations can be nearly scale-invariant, while isocurvature perturbations are blue-tilted.

From eq. (3.18) we find that the spectrum of isocurvature perturbations can be blue-tilted for the coupling  $g$  with  $g \gtrsim m_\phi/M_p$ . In Fig. 5 we plot the spectra of  $P_{\mathcal{R}}$ ,  $P_S$  and  $P_C$  for two cases with  $\beta = 0.01$  and  $\beta = 0.95$ . Note that in these cases the model parameters are chosen so that  $\mu_s^2$  is positive during the whole of double inflation. When  $\beta = 0.01$ , the spectrum of isocurvature perturbations is slightly blue-tilted, while for  $\beta = 0.95$  it is highly blue-tilted.

The two spectra  $P_{\mathcal{R}}$  and  $P_C$  are not significantly modified by the presence of a coupling term  $g$ . It can be understood that the correlation of adiabatic and isocurvature perturbations gets smaller as  $\chi$  approaches the potential valley with decreasing  $\dot{\theta}$ . As shown in Fig. 5 the correlation  $r_C$  tends to decrease more on smaller scales as we choose larger values of  $\beta$ . When  $\beta \gtrsim 1$  we find that  $r_C$  decreases rapidly on smaller scales, which is associated with the highly blue-tilted spectrum of isocurvature perturbations. This is confirmed by the definition of  $r_C$  in eq. (2.36) where only  $P_S$  increases toward smaller scales.

From Fig. 5 we find that the two consistency relations (2.41) and (2.42) do not show good agreement with  $r_T$  obtained by eq. (2.37), especially for larger scales. This is caused by the violation of the slow-roll conditions at horizon crossing and also by the change of  $\mu_Q^2/(3H^2)$ ,  $\mu_s^2/(3H^2)$  and  $\dot{\theta}/H$  during inflation. Since the correlation decreases toward smaller scales, the disagreement tends to be weaker for smaller  $N_k$  in this case of the first consistency relation. Since the second consistency relation is affected by the change of the mass terms after horizon crossing, it does not agree well with numerical results even on smaller scales.

Note that in Fig. 5 the strength of the correlation  $r_C$  increases for larger  $\beta$  around the scale  $N_H = 60$ . Since the inclusion of the coupling  $g$  provides the additional source term for  $\dot{\theta}$  [see the  $\eta_{\phi\chi}$  term in eq. (2.23)], this works to induce the larger correlation as long as  $\chi$  is not strongly suppressed. Making use of eq. (2.23), we can easily show that the correlation is nonzero even for  $R = 1$ .<sup>8</sup> Fig. 6 indicates that the values of  $r_C$  are increased around the region where the correlation is strong, by including the coupling  $g$ .

If the condition,  $m_\phi^2\phi^2 + m_\chi^2\chi^2 < 2g^2\phi^2\chi^2$ , is satisfied at horizon crossing, the mass of  $\delta s$  is *negative*. So the spectrum of isocurvature perturbations produced is red tilted with a steeper slope than in the case of  $g = 0$ . Fig. 7 corresponds to the case where the spectrum  $P_S$  is red-tilted for  $57 \lesssim N_k \lesssim 63$  but begins to be blue-tilted for  $N_k \lesssim 57$ . The negative mass of  $\delta s$  leads to the red-tilted spectrum on large scales as expected. When  $\phi$  and  $\chi$  are the same order on these scales, the correlation  $r_C$  can be close to unity [see the right panel of Fig. 7]. When the mass of  $\delta s$  becomes positive and  $\chi$  begins to decrease toward  $\chi = 0$ , the situation is almost the same as discussed previously. In this case we have highly blue-tilted spectrum for isocurvature perturbations with suppressed correlations ( $r_C \ll 1$ ).

Unless  $g$  is extremely small ( $g \ll m_\phi/M_p$ ), then it is natural to have a stage of the negative  $\mu_s^2$  during double inflation. For example, when  $g \gtrsim m_\phi/M_p$ , it is easy to satisfy the condition,  $\mu_s^2 < 0$ , if  $\chi$  is larger than the order of the Planck mass. For the double inflationary scenario where inflation starts out with large initial values of  $\phi$  and  $\chi$  much greater than the Planck mass, the spectrum  $P_S$  is highly red-tilted. Nevertheless, when  $g$  is large and  $\beta \gg 1$ ,  $\chi$  decreases very rapidly toward  $\chi = 0$ . Therefore the blue-tilted spectrum of  $P_S$  immediately appears once the mass of  $\delta s$  becomes positive.

We have found that a variety of power spectra and correlations can be obtained, depending on the initial values of scalar fields and the parameters of the model. In particular the inclusion of the coupling  $g$  leads to an interesting power spectrum of isocurvature perturbations that tend to increase toward large scales (corresponding to  $\mu_s^2 < 0$ ) and also grow again toward smaller scales (corresponding to  $\mu_s^2 > 0$ ). If such a spectrum is supported from observations, it

<sup>7</sup>When  $\beta \gg 1$  the spectrum of isocurvature perturbations is highly blue-tilted. This is actually the case for the preheating scenario where large-scale entropy field perturbations are strongly suppressed for the coupling  $g$  required for strong preheating, see refs. [36].

<sup>8</sup>We have  $r_C = 0$  for  $R = 1$  and  $\phi = \chi$ .

should be possible to constrain on the strength of the coupling  $g$  and other model parameters by taking into account the information of the correlation  $r_C$  as well.

There exist other models of double inflation which provide the  $\beta H^2$  correction as in eq. (3.18). One such model is a non-minimally coupled  $\chi$  field with a minimally coupled field  $\phi$  [18]:

$$V = \frac{1}{2}m_\phi^2\phi^2 + \frac{1}{2}m_\chi^2\chi^2 + \frac{1}{2}\xi R\chi^2, \quad (3.20)$$

where  $\xi$  is a non-minimal coupling between the scalar curvature  $R$  and the field  $\chi$ . In this model the spectrum of the isocurvature perturbations is red-tilted due to the amplification of  $\delta\chi$  for negative  $\xi$  [28,32], while it is blue-tilted for positive  $\xi$ . Although the decomposition into adiabatic and entropy “fields” is not as simple as in the case of minimally coupled fields discussed in Sec. II, it would be of interest to extend our analysis to this case.

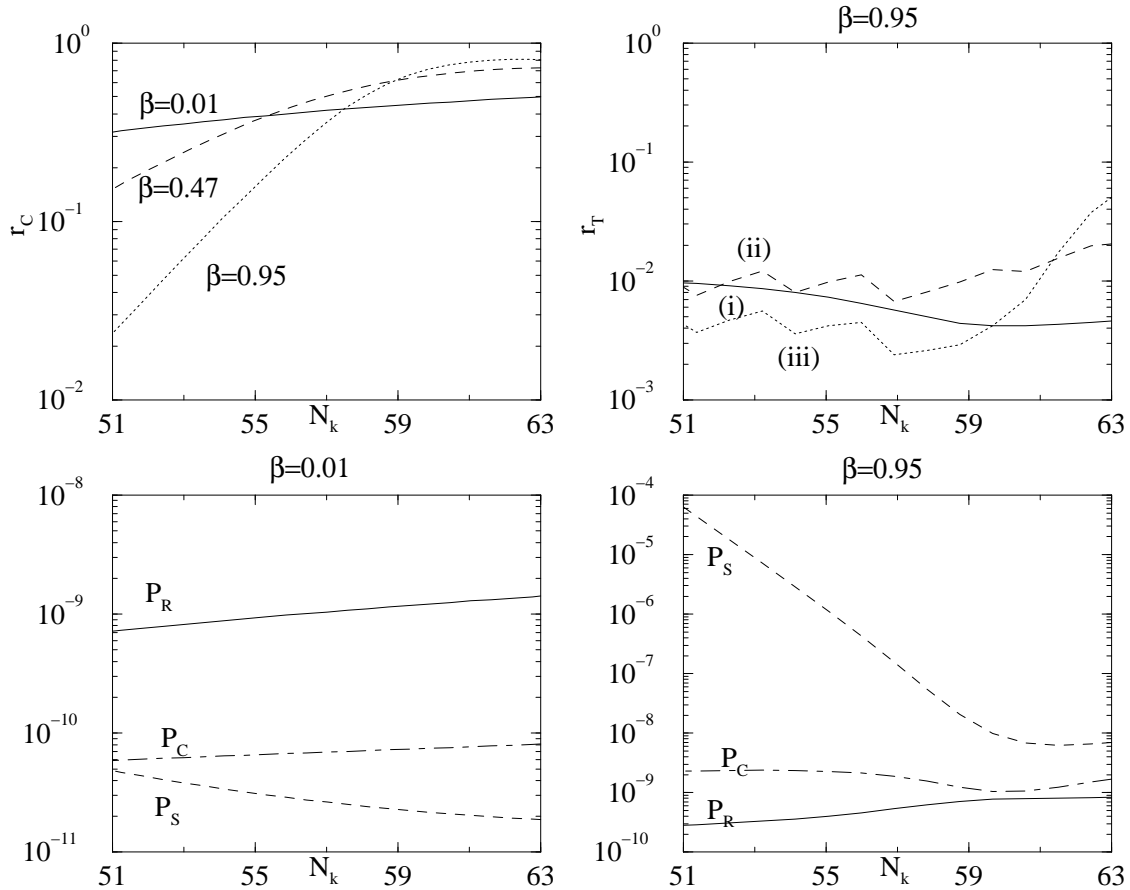


FIG. 5: The spectra of the correlation  $r_C$  for  $\beta = 0.01, 0.47, 0.95$ , and the ratio  $r_T$  which are derived by eqs. (2.37), (2.41) and (2.42), denoted by (i), (ii), and (iii), respectively. The model parameters are chosen to be  $R = 3$ ,  $m_\phi = 5.0 \times 10^{-7} M_p$ , and  $\phi = 3.2 M_p$ ,  $\chi = 0.3 M_p$  at  $N_k = 65$ . The power spectra  $P_R$ ,  $P_S$ , and  $P_C$  are also shown for  $\beta = 0.01$  (left) and  $\beta = 0.95$  (right).

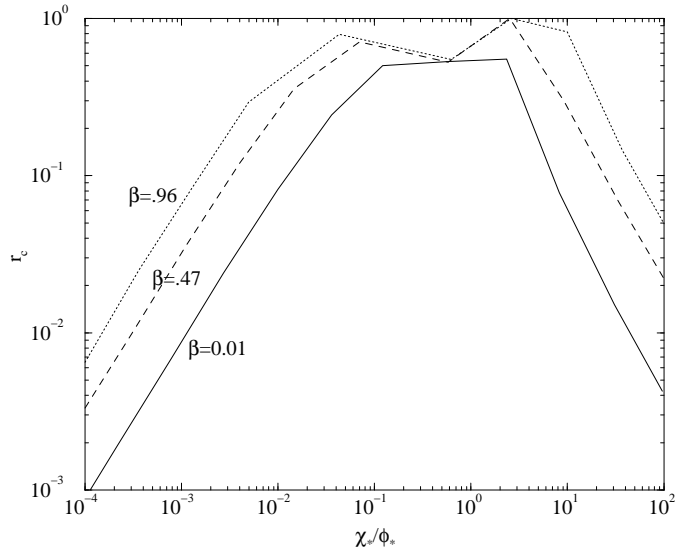


FIG. 6: The correlation  $r_C$  as a function of  $\chi_*/\phi_*$  for  $\beta = 0.01, 0.47, 0.95$  on the scale corresponding to  $N_k = 60$ . The model parameters are the same as in Fig. 5.

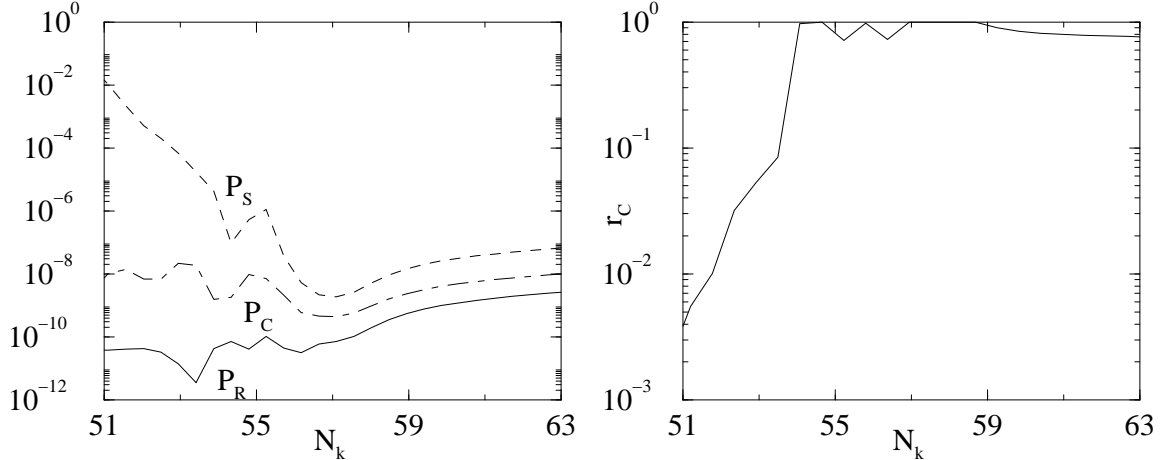


FIG. 7: The power spectra  $P_R, P_S, P_C$  (left) and the correlation  $r_C$  for  $R = 3, m_\phi = 2.0 \times 10^{-7} M_p$  and  $g = 2.0 \times 10^{-6}$  (corresponding to  $\beta = 23.9$ ).

#### IV. DOUBLE INFLATION MOTIVATED BY SUPERSYMMETRY

We now come to the perhaps the most interesting of the models we have studied. In hybrid and supernatural inflationary models [43,44,45], the symmetry breaking transition occurs in the presence of the second scalar field,  $\chi$ . The effective potential of the original hybrid inflation model is given by [43]

$$V = \frac{\lambda}{4} \left( \chi^2 - \frac{M^2}{\lambda} \right)^2 + \frac{1}{2} g^2 \phi^2 \chi^2 + \frac{1}{2} m^2 \phi^2. \quad (4.1)$$

This potential is closely related with those obtained in supersymmetric theories [45] - [51]. For example, consider the supersymmetric theory with a superpotential

$$W = S (\kappa_0 \varphi \bar{\varphi} - \mu^2) , \quad (4.2)$$

which includes two superfields,  $S$ ,  $\varphi$ , together with a conjugate pair,  $\bar{\varphi}$ . In the global supersymmetric limit ( $M_p \rightarrow \infty$ ), one obtains the following effective potential for two superfields  $S$  and  $\varphi$ :

$$V = |\kappa_0 \varphi \bar{\varphi} - \mu^2|^2 + \kappa_0^2 |S|^2 (|\varphi|^2 + |\bar{\varphi}|^2) + D\text{-terms} . \quad (4.3)$$

Note that this has a potential minimum at  $|S| = 0$ ,  $\langle \varphi \rangle \langle \bar{\varphi} \rangle = \mu^2 / \kappa_0$ ,  $|\langle \varphi \rangle| = |\langle \bar{\varphi} \rangle|$ . Making gauge and  $R$ -transformations in the  $D$ -flat direction,  $|\langle \varphi \rangle| = |\langle \bar{\varphi} \rangle|$ , the complex superfields,  $S$ ,  $\varphi$ ,  $\bar{\varphi}$  can be replaced by real scalar fields,  $\phi$  and  $\chi$ , as

$$S = \phi / \sqrt{2}, \quad \varphi = \bar{\varphi} = \chi / 2. \quad (4.4)$$

Then the potential (4.3) yields

$$V = \frac{\kappa_0^2}{16} \left( \chi^2 - \frac{4\mu^2}{\kappa_0} \right)^2 + \frac{1}{4} \kappa_0^2 \phi^2 \chi^2 , \quad (4.5)$$

where we neglected the  $D$ -terms. The absolute minimum appears at  $\phi = 0$ ,  $\chi = 2\mu / \sqrt{\kappa_0}$ . When  $\phi > 2\mu / \sqrt{\kappa_0}$ , the potential is exactly flat at the local minimum,  $\phi = 0$ . Adding a mass term  $\frac{1}{2} m^2 \phi^2$  in Eq. (4.5) results in the effective potential (4.1) with replacement,  $\kappa_0^2 / 2 = g^2 = 2\lambda$  and  $\mu^2 = M^2 / (2\sqrt{\lambda})$ . Therefore the supersymmetric version of the hybrid or double inflation corresponds to the case with  $g^2 / \lambda = 2$ .

Taking into account the supergravity correction gives rise to a slowly varying effective potential for  $\phi > 2\mu / \sqrt{\kappa_0}$ , whose form is approximately given by  $V \simeq \mu^4 [1 + \phi^4 / (8M_p^4)]$  [50]. If one-loop radiative corrections are included, the total effective potential for  $\phi > 2\mu / \sqrt{\kappa_0}$  involves logarithmic term,  $\ln \phi$ , as well as the  $\phi^4$  term [51]. The corrections terms,  $\phi^4$  or  $\ln \phi$ , can lead to an inflationary expansion of the universe for  $\phi > 2\mu / \sqrt{\kappa_0}$ .

Although these are different from the mass term  $\frac{1}{2} m^2 \phi^2$  in eq. (4.1), the basic structures of the models motivated by supersymmetric theories are well described by the potential (4.1). In particular, when we discuss the correlation between adiabatic and isocurvature perturbations, the crucial point is the evolution of scalar fields *after* the symmetry breaking phase rather than the early evolution at  $\phi > 2\mu / \sqrt{\kappa_0}$ . Therefore we shall consider the model (4.1) in order to understand the basic properties of the correlations. We are particularly interested in the supersymmetric case with  $g^2 / \lambda = 2$ .

### A. The condition for double inflation and the background evolution

We shall first consider the evolution of the background and the condition for double inflation to take place (rather than just a single phase of inflation) for the model (4.1). When  $\phi$  is larger than  $\phi_c \equiv M/g$ , inflation takes place due to the slow-roll evolution of  $\phi$ . Since the mass of  $\chi$  is positive for  $\phi > \phi_c$ , the field  $\chi$  rolls down to the potential valley at  $\chi = 0$ . Therefore the potential is approximately described as  $V \simeq \frac{M^4}{4\lambda} + \frac{1}{2} m^2 \phi^2$ . If the condition,  $m^2 \phi_c^2 \ll M^4 / \lambda$ , is satisfied, the Hubble constant at  $\phi = \phi_c$  is given by  $H \simeq H_0 \equiv \sqrt{2\pi / (3\lambda)} M^2 / M_p$ . Let us denote the masses of the two fields  $\phi$  and  $\chi$  relative to  $H_0^2$  as  $\gamma$  and  $\delta$ :

$$\gamma \equiv \frac{m^2}{H_0^2} = \frac{3\lambda m^2 M_p^2}{2\pi M^4}, \quad \delta \equiv \frac{g^2 \phi^2 - M^2}{H_0^2} = \frac{3\lambda}{2\pi} \left( \frac{M_p}{M} \right)^2 (c^2 - 1), \quad (4.6)$$

where we set  $\phi = c\phi_c$ .  $\gamma$  is required to be smaller than unity in order to lead to the first stage of inflation for  $\phi > \phi_c$ , thereby yielding

$$M^2 \gtrsim m M_p \sqrt{\lambda}. \quad (4.7)$$

Whether the second stage of inflation occurs or not after  $\phi$  drops below  $\phi_c$  depends on the model parameters. If the ‘‘water-fall’’ condition,

$$M^3 \ll \lambda m M_p^2, \quad (4.8)$$

is satisfied, inflation soon comes to an end after the symmetry breaking. This corresponds to the original version of the hybrid inflationary scenario where inflation ends due to the rapid rolling of the field  $\chi$  [43].

Combining eqs. (4.7) and (4.8), one has  $M \gg m$  and

$$\delta \gg \frac{M}{m}(c^2 - 1) \gg c^2 - 1. \quad (4.9)$$

This means that the classical field  $\chi$  is strongly suppressed for  $\phi > \phi_c$  ( $\chi \propto a^{-3/2}$ ). Since inflation typically starts when the value of  $c^2 - 1$  is of order unity or much larger than unity, it is inevitable to avoid the suppression of  $\chi$  when the water-fall condition is satisfied. Note that  $\delta$  changes sign after the symmetry breaking. The field  $\chi$  and its large-scale fluctuations are amplified by the tachyonic instability associated with negative  $\chi$  mass [56,57,58,59].

Although the growth is strong for large-scale modes ( $k \rightarrow 0$ ), the size of these fluctuations is vanishingly small at the beginning of the tachyonic instability due to their exponential suppression for  $\phi > \phi_c$ . Therefore the small-scale modes that are not significantly suppressed for  $\phi > \phi_c$  provide the larger contribution to the total variance  $\langle \chi^2 \rangle$  of  $\chi$  rather than the large-scale modes.

The condition for the second stage of inflation to occur is characterised by  $|\delta| \ll 1$ , namely

$$M^2 \gg \lambda M_p^2. \quad (4.10)$$

In this case the field  $\chi$  and its large-scale perturbation are free from the inflationary suppression for  $\phi > \phi_c$ , unless inflation starts out with very large values of  $\phi$  satisfying  $c \gg 1$ . Note that one has  $m^2/M^2 \ll g^2/\lambda$  under the condition that the first stage of inflation is driven by the Hubble constant,  $H_0$  (namely,  $m^2\phi_c^2 \ll M^4/\lambda$ ).

Therefore one has  $M \gg m$  for  $g^2/\lambda = \mathcal{O}(1)$ . Combining this relation with eq. (4.10) gives  $M^3 \gg \lambda m M_p^2$ , which means that the water-fall condition (4.8) is violated. In this case the evolution of the field  $\chi$  is sufficiently slow so that the second stage of inflation occurs after the symmetry breaking.

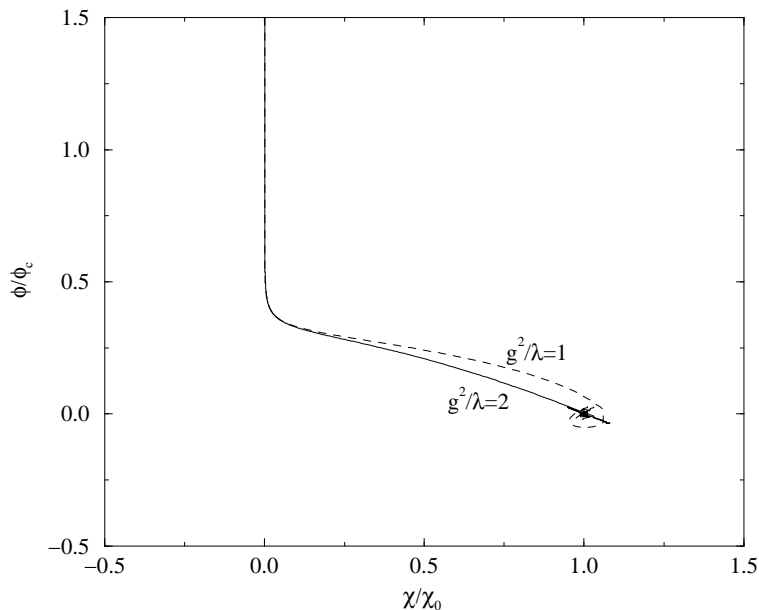


FIG. 8: The trajectory of two scalar fields in the plane  $(\phi/\phi_c, \chi/\chi_0)$ . Model parameters are chosen to be  $M = 7.0 \times 10^{-7} M_p$ ,  $m = 2.0 \times 10^{-7} M_p$  with initial scalar fields  $\phi_i = 1.5\phi_c$  and  $\chi_i = 10^{-3}\chi_0$ . We show two cases of  $g^2/\lambda = 1$  and  $g^2/\lambda = 2$  with  $\lambda = 10^{-12}$ . The trajectories are curved in field space, which means that  $\dot{\theta} \neq 0$ .

Let us consider the evolution of the background for  $g^2/\lambda = \mathcal{O}(1)$ . The number of e-folds during the first stage of inflation is described as

$$N_1 \simeq \kappa^2 \int_{\phi_c}^{\phi_i} \frac{V}{V'} d\phi \simeq \frac{2\pi M^4}{\lambda m^2 M_p^2} \ln \frac{\phi_i}{\phi_c}, \quad (4.11)$$

where we used  $V \simeq \frac{M^4}{4\lambda} + \frac{1}{2}m^2\phi^2$  for  $\phi > \phi_c$ . Here  $\phi_i$  is the value of  $\phi$  at the beginning of double inflation. Note that we have  $N_1 \gg 1$  under the condition of eq. (4.7) [i.e.,  $\gamma \ll 1$ ]. Similarly the number of e-folds after the symmetry breaking is approximately expressed as

$$N_2 \simeq \kappa^2 \int_{\chi_0}^{\chi_c} \frac{V}{V'} d\chi \simeq \frac{2\pi M^2}{\lambda M_p^2} \ln \frac{\chi_0}{\chi_c}, \quad (4.12)$$

where we used  $V \simeq \frac{\lambda}{4} \left( \chi^2 - \frac{M^2}{\lambda} \right)^2$ . Here  $\chi_0 = M/\sqrt{\lambda}$  and  $\chi_c$  is the value of  $\chi$  at  $\phi = \phi_c$ . Again  $N_2 \gg 1$  is satisfied under the condition of eq. (4.10). We are interested in the double inflationary scenario where the total amount of e-folds,  $N_T = N_1 + N_2$ , exceeds  $N_H = 60$ .

When  $g^2/\lambda = \mathcal{O}(1)$ , the critical value  $\phi_c = M/g$  and the potential minimum  $\chi_0 = M/\sqrt{\lambda}$  are of the same order. Two fundamental masses around the potential minimum are characterised by  $m_\phi \equiv (g/\sqrt{\lambda})M$  and  $m_\chi \equiv \sqrt{2}M$ . Therefore these masses are also comparable when  $g^2/\lambda = \mathcal{O}(1)$ . In particular in the supersymmetric case with  $g^2/\lambda = 2$ , the two masses are completely equal.

In this case the trajectory of the two scalar fields after the symmetry breaking is close to a straight line in the  $(\phi/\phi_c, \chi/\chi_0)$  plane if the velocities of  $\phi$  and  $\chi$  are sufficiently small at the bifurcation point,  $\phi = \phi_c$  [60]. However, since  $\dot{\phi}$  is non-zero because of the non slow-roll evolution around  $\phi = \phi_c$ , the trajectory is not strictly described by a straight line after the symmetry breaking. In fact this behaviour can be found in our numerical simulation in Fig. 8. When  $g^2/\lambda = \mathcal{O}(1)$  and  $g^2/\lambda \neq 2$  the two scalar fields exhibit chaotic behaviour as shown in refs. [60,61,62]. The trajectory in the  $g^2/\lambda = 1$  case is illustrated in Fig. 8.<sup>9</sup> Since the trajectory of the two scalar fields is generally curved, this leads to the variation of  $\theta$  in field space ( $\dot{\theta} \neq 0$ ), thereby generating a correlation of perturbations for  $\phi < \phi_c$ . Note that in the case of  $g^2/\lambda \ll 1$  or  $g^2/\lambda \gg 1$ ,  $m_\phi$  and  $m_\chi$  as well as  $\phi_c$  and  $\chi_0$  take quite different values. We will not consider such cases in this work, since we are interested in the double inflation motivated by supersymmetric theories.

## B. Perturbations

Let us next analyze the perturbations and correlations in the double inflation model with potential (4.1). When the field  $\phi$  evolves slowly along the potential valley with  $\chi = 0$  before the symmetry breaking, the spectral index of the curvature perturbation generated in the first stage of double inflation can be estimated by eq. (2.32), as

$$n_{\mathcal{R}} - 1 \simeq -6\epsilon_\phi + 2\eta_{\phi\phi} \simeq \frac{2}{3} \gamma \left( 1 - \frac{3m^2\phi^2}{V} \right), \quad (4.13)$$

where  $\gamma$  is defined by eq. (4.6). When the condition,  $m^2\phi^2 \ll V \simeq M^4/(4\lambda)$ , holds as is the case with the original hybrid inflation scenario [43], one has the blue-tilted spectrum with  $n_{\mathcal{R}} - 1 \simeq \frac{2}{3} \gamma > 0$ . Similarly the spectral index of the isocurvature perturbation generated for  $\phi > \phi_c$  is given as

$$n_S - 1 \simeq -2\epsilon_\phi + 2\eta_{\chi\chi} \simeq \frac{2}{3} \delta - \gamma \frac{m^2\phi^2}{3V}, \quad (4.14)$$

where we used eq. (2.33). Therefore when the condition,  $\frac{2}{3}\delta > \gamma \frac{m^2\phi^2}{3V}$ , is satisfied, the isocurvature perturbation is also blue-tilted. Note that the spectral index of the correlation  $P_C$  is similar to that of  $P_S$  except for the last term in eq. (2.34) that is of order  $1/N_k \ll 1$  when  $|\zeta_k N_k| \ll 1$ .

The spectral indices in eqs. (4.13) and (4.14) can be modified in the presence of the tachyonic instability region with  $\phi < \phi_c$ . After the symmetry breaking, the field perturbation  $\delta\chi$  begins to be amplified due to the negative  $\chi$  mass in eq. (4.6) with  $c < 1$ . This growth is accompanied with the amplification of the entropy field perturbation  $\delta s$  for small  $k$  modes, which stimulates the enhancement of large-scale curvature perturbations by the relation (2.25) [see Fig. 9].

As shown in Fig. 9,  $|\dot{\theta}/H|$  decreases during the first stage of inflation, but begins to increase after the symmetry breaking. This can lead to the strong correlation between adiabatic and isocurvature perturbations. In fact once  $\delta s$

---

<sup>9</sup>Note that the amplitude of the two scalar fields can be higher as in ref. [62,60] by changing model parameters.

and  $|\dot{\theta}/H|$  grow sufficiently, this works as source terms for  $Q$  in the r.h.s. of eq. (2.14), thereby stimulating the growth of  $\Phi$  through the relation (2.12). This behaviour is clearly seen in the numerical simulation of Fig. 9.

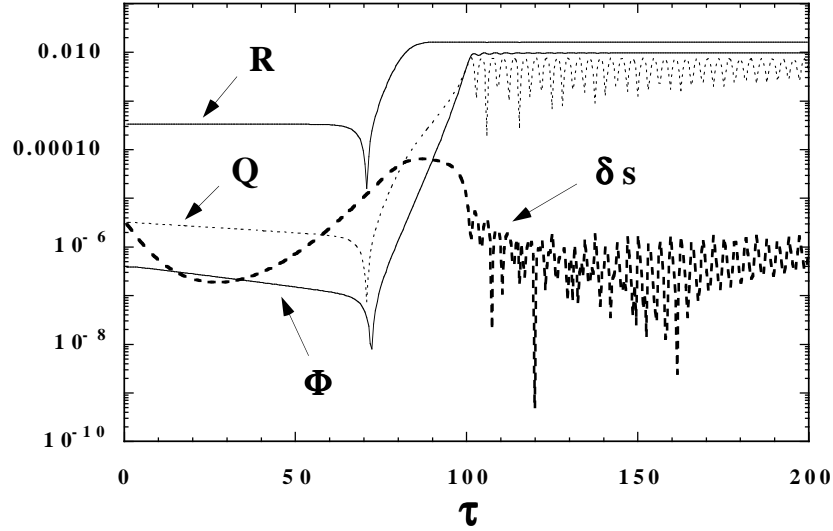


FIG. 9: The evolution of  $\mathcal{R}$ ,  $\Phi$ ,  $\delta s$  and  $Q$  for a mode which left the horizon before 60 e-foldings from the end of the double inflation. Model parameters are  $g^2/\lambda = 2$ ,  $g = 1.5 \times 10^{-10}$ ,  $M = 5.0 \times 10^{-6}$  and  $m = 0.2M$  with initial conditions,  $\phi = 1.34\phi_c$  and  $N = 10^{-3}\chi_0$ .  $\mathcal{R}$  and  $\Phi$  are amplified due to the tachyonic growth of  $\delta s$  and  $Q$  during the second stage of inflation.

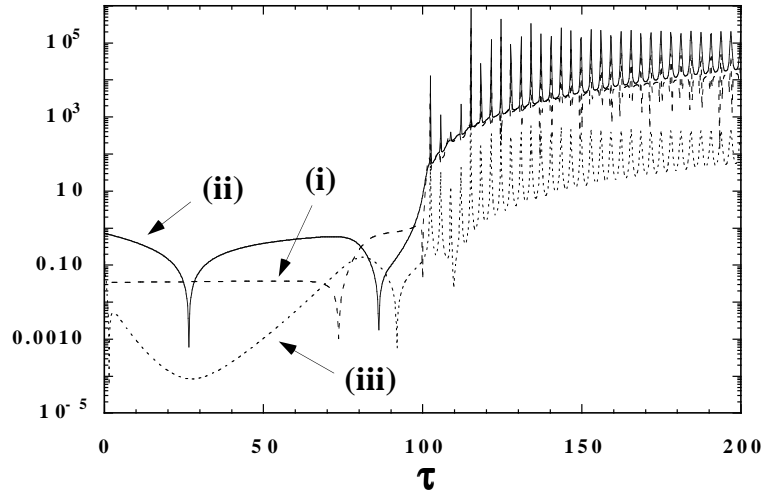


FIG. 10: The evolution of (i)  $|\mu_Q^2/(3H^2)|$ , (ii)  $|\mu_s^2/(3H^2)|$  and (iii)  $|\dot{\theta}/H|$  for  $g^2/\lambda = 2$ ,  $g = 1.5 \times 10^{-10}$ ,  $M = 5.0 \times 10^{-6}$  and  $m = 0.2M$  with initial conditions,  $\phi = 1.34\phi_c$  and  $\chi = 10^{-3}\chi_0$ . Although we showed the absolute values of these quantities, it happens that these take negative values in the tachyonic instability region.

Let us consider the spectra of perturbations at the end of the double inflation. In Fig. 11 we show the spectra  $P_R$ ,  $P_S$ , and  $P_C$  around the scale  $N_H = 60$  for three different cases. The case (a) corresponds to the one with  $\gamma \simeq 0.08 \ll 1$

and  $\delta \simeq c^2 - 1 \simeq 1$  around  $N_k \sim 60$ , in which case from eqs. (4.13) and (4.14) one has a slight blue-tilt for  $P_{\mathcal{R}}$  and a rather steep blue-tilt for  $P_S$  at the end of the *first* stage of the double inflation.

In fact we have numerically checked that such spectra are generated before symmetry breaking. However these are different from the final spectra obtained at the end of double inflation. Since the strong conversion between adiabatic and isocurvature perturbations occurs during the tachyonic instability region, the final spectrum of curvature perturbations is affected by the steep blue-tilted spectrum of isocurvature perturbations. Therefore the final  $P_{\mathcal{R}}$  exhibits the steeper blue-tilted spectrum than predicted by eq. (4.13).

This tells us that the correlation between adiabatic and isocurvature perturbations is important to correctly estimate the final spectra. The slow-roll results (4.13) and (4.14) typically show limitations when the correlation is strong. Note that in Fig. 11 all spectra  $P_R$ ,  $P_S$ , and  $P_C$  in the case (a) exhibit almost the same blue spectral indices due to the strong correlation.

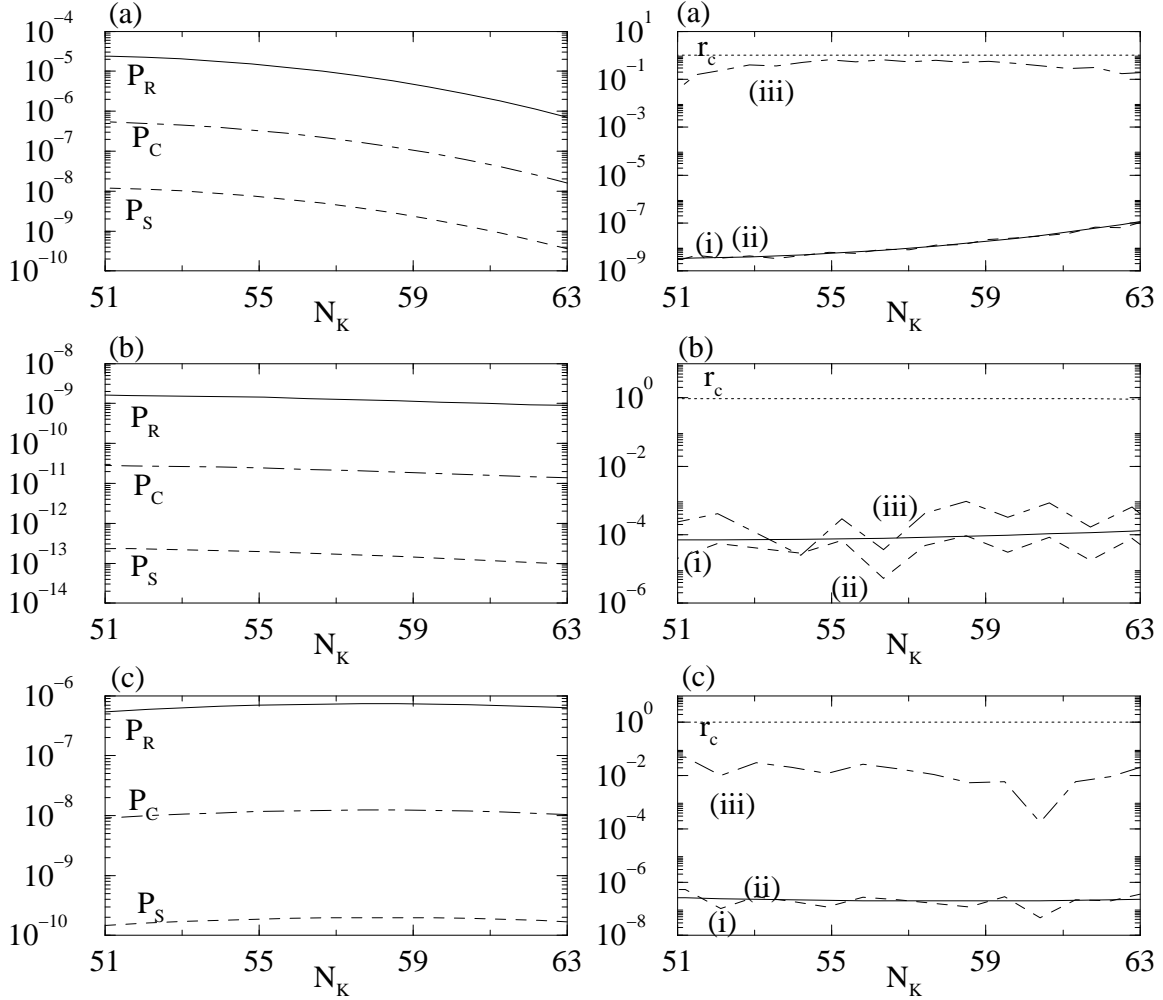


FIG. 11: The power spectra  $P_R$ ,  $P_S$  and  $P_C$  (left panel) for  $g^2/\lambda = 2$ . Each case corresponds to (a)  $M = 7.0 \times 10^{-7} M_p$ ,  $\lambda = 1.0 \times 10^{-12}$ ,  $m = 2.0 \times 10^{-7} M_p$ ,  $\phi_i = 1.47\phi_c$ ,  $\chi_i = 1.0 \times 10^{-3}\chi_0$ , (b)  $M = 8.5 \times 10^{-7} M_p$ ,  $\lambda = 9.0 \times 10^{-13}$ ,  $m = 2.0 \times 10^{-7} M_p$ ,  $\phi_i = 1.22\phi_c$ ,  $\chi_i = 5.0 \times 10^{-2}\chi_0$ , (c)  $M = 8.1 \times 10^{-7} M_p$ ,  $\lambda = 1.0 \times 10^{-12}$ ,  $m = 2.0 \times 10^{-7} M_p$ ,  $\phi_i = 1.11\phi_c$ ,  $\chi_i = 1.0 \times 10^{-3}\chi_0$ . The right panel shows the correlation  $r_c$  and the ratio  $r_T$  that are derived by using eq. (2.36), and two consistency relations (2.41) and (2.42), which are denoted by (i), (ii), (iii), respectively. Note that in the case (2.42) we have taken the absolute value of  $r_T$ .

Although the case (a) corresponds to the one with rather steep blue-tilted spectra, one can obtain nearly scale-invariant spectra by choosing small values of  $\gamma$  and  $\delta$  relative to unity. For example the case (b) in Fig. 11 corresponds to the one with  $\gamma \simeq 0.04 \ll 1$  and  $\delta \simeq 0.6(c^2 - 1) \lesssim 0.2$  for  $N_k \lesssim 63$ .

In this case both the adiabatic and isocurvature spectra generated for  $\phi > \phi_c$  are slightly blue-tilted, as predicted by eqs. (4.13) and (4.14). The conversion of perturbations occurs after the symmetry breaking as well, but the spectral indices are mostly inherited by the end of double inflation because both  $P_{\mathcal{R}}$  and  $P_S$  have similar small spectral indices at  $\phi = \phi_c$ . As shown in Fig. 11 all of  $P_R$ ,  $P_S$ , and  $P_C$  exhibit a slightly blue-tilted spectra at the end of double inflation.

One may consider that the tachyonic growth of large-scale perturbations may lead to the red-tilted spectra. In the cases (a) and (b) all modes shown in Fig. 11 (corresponding to  $51 \lesssim N_k \lesssim 63$ ) already left far outside of the horizon when the field reaches  $\phi = \phi_c$ . Since the physical momenta satisfy  $k/a \ll H$  for these all modes, the tachyonic growth rate of perturbations is practically the same for the modes corresponding to  $51 \lesssim N_k \lesssim 63$ . Therefore in the cases (a) and (b) the presence of the tachyonic region does not yield the red-tilted spectra.

However, if the duration in the first stage of inflation is short, it is possible to obtain the red-tilted spectrum on smaller scales. For example, in the case (c) illustrated in Fig. 11, the e-folds during the first stage of inflation are  $N \sim 7.5$  (the total e-folds are  $N \sim 65$ ). The modes corresponding to  $N_k \gtrsim 58$  crossed the horizon before the field reaches to the point  $\phi = \phi_c$ . For these modes the spectra of perturbations are blue-tilted as are the cases of (a) and (b).

In contrast, the smaller-scale modes with  $N_k \lesssim 58$  crossed the horizon after the symmetry breaking, in which case one has the red-tilted spectrum due to the negative  $\chi$  mass [see Fig. 11]. The case (c) corresponds to the slightly red-tilt spectra with  $|\delta| \ll 1$ . If the values of  $|\delta|$  are increased, we have steeper negative tilts than shown in Fig. 11. It is very interesting that such a variety of spectra can be obtained by different choices of model parameters and initial conditions.

In Fig. 10 we find that the absolute values of the mass  $\mu_s^2/(3H^2)$  and  $\dot{\theta}/H$  change during the double inflation, while the variation of  $\mu_Q^2/(3H^2)$  is small. In addition, although the mass  $\mu_s^2/(3H^2)$  is positive initially, it changes sign after the symmetry breaking. Therefore, to use the ‘‘frozen’’ positive mass in eq. (2.20) is not typically valid, thereby leading to the errors in the final consistency relations. And while the correlation is suppressed for  $\phi > \phi_c$ , the tachyonic growth of the fluctuation  $\delta\chi$  yields the strong correlation after the symmetry breaking.

Numerically we found that the correlation ratio,  $r_C$ , is very close to unity at the end of double inflation (see Fig. 11). This is associated with the enhancement of  $\mathcal{R}$  and  $\Phi$  shown in Fig. 9. In Fig. 11 the first consistency relation shows very good agreement with the numerical result in the cases (a) and (c), while the case (b) is not so good. In the cases (a) and (c) we chose the initial  $\chi$  value  $\chi_i = 10^{-3}\chi_0$ , while the case (b) corresponds to  $\chi_i = 0.05\chi_0$ . In the former cases one has  $\dot{\theta}/H$  of order 0.001 around the scale  $N_k \sim 60$ , but  $\dot{\theta}/H$  is larger by more than one order of magnitude in the latter case. The correlation is negligible at horizon crossing in the cases (a) and (c), but in case (b) it is not. This is the main reason of the deviation from the first consistency relation in the case (b). In fact we have numerically checked that the first consistency relation tends to agree with the numerical results as we decrease the initial  $\chi$  (i.e., smaller  $\dot{\theta}/H$ ).

Our numerical simulations show that the second consistency relation does not agree with the one obtained by the definition (2.37) [see Fig. 11]. In particular, although  $r_T$  is defined to be positive-definite in eq. (2.36), negative values of  $r_T$  appear when we use eq. (2.42), implying strong deviations from the second consistency relation [Note that in Fig. 11 we showed the absolute values of  $r_T$ ]. Again this is mainly due to the violation of the assumption of the constant masses and  $\dot{\theta}/H$  during the tachyonic instability region.

Notice also that if we use the slow-roll expression for  $x$  in eq. (2.39) this does not provide the correct value of the correlation  $r_C$ . In the case (a) of Fig. 11, for example, we have  $(\dot{\theta}/H)_k \sim 0.001$  and  $\zeta_k \sim 0.37$  around  $N_k = 60$ . Therefore eq. (2.39) leads to  $x \sim 0.005$  and  $r_C \sim 0.005 \ll 1$ . This is significantly different from the numerical value of  $r_C$  close to unity. We have to integrate the  $\dot{\theta}/H$  term from the horizon crossing to the end of inflation in order to correctly estimate the final value of  $r_C$ . Note that when we evaluate  $x$  in eq. (2.38) numerically the first consistency shows excellent agreement with the numerical results [like in the cases (a) and (c) in Fig. 11], as long as the correlation is not large at horizon crossing.

When the  $\chi$  mass is light ( $|\delta| \lesssim 1$ ) and the second phase of inflation takes place, we found that the correlation  $r_C$  is close to one, even changing the values of  $g^2/\lambda$  to of order unity. The correlation is also expected to be strong in other models of double inflation with a tachyonic instability region.

## V. CONCLUSIONS

In this paper we have studied the correlation of adiabatic and isocurvature perturbations generated in inflationary scenarios with two phases of inflation (double inflation). We have made a detailed multi-parameter numerical analysis

of the power spectra relevant for the cosmic microwave background and large-scale structure. We also studied the validity of the inflationary consistency relations derived from slow-roll analysis for two different models of the double inflation – the noninteracting/interacting two massive scalar fields and the supersymmetric model with a tachyonic (spinodal) instability separating the two phases of inflation.

In single-field inflationary scenarios, the slow-roll approximation is typically a reliable apart except near the end of inflation which is usually not important observationally. In the case of multiple scalar fields, however, there exist some limitations in the use of slow-roll results since the slow-roll parameter of a heavy scalar field is already large around the end of the first stage of inflation.

In addition, the assumption of the slow variation of the effective masses of “adiabatic” and “entropy” fields, which is used to obtain the spectra of perturbations analytically, is often not valid in the context of the double inflationary scenarios. This is reflected in our results where we found that the slow-roll derived correlation  $r_C$  and three spectral indices  $n_{\mathcal{R}}, n_S, n_C$  do not agree with the full numerical simulations, especially when the correlation is strong. If the correlation is negligibly small *at horizon crossing*, the first consistency relation (2.41) shows good agreement with our numerical results [see the cases (a) and (b) in Fig. 3 and the cases (a) and (c) in Fig. 11]. This is consistent with the result of Wands *et al.* that the first consistency relation was obtained by only assuming a vanishingly small correlation at horizon crossing [34]. However, in the case where slow-roll conditions are violated at horizon crossing, which can occur in double inflationary scenarios, we find that numerical results exhibit some deviation from the first consistency relation (2.41) [see the case (c) in Fig. 3 and the case (b) in Fig. 11]. The second consistency relation (2.42) is more strongly affected by the change of the entropy/adiabatic mass and the scalar field velocity angle  $\theta$  during double inflation, thereby showing the stronger deviation especially when the correlation is large. These suggest the necessity of numerical analysis – or a refined analytical treatment – in order to correctly estimate the final power spectra, spectral indices and the correlations of perturbations.

We have also found that a wide variety of power spectra and correlations can be obtained, depending on the parameters of the models considered. In the case of noninteracting massive scalar fields, two important quantities determine the strength of the correlation: the ratio of the two scalar fields ( $\tan \alpha_*$ ) and the ratio of the two masses ( $R$ ). We made a complete classification for several different cases to understand the correlation appropriately.

When the interaction between two scalar fields ( $g^2\phi^2\chi^2$ ) is introduced, this can lead to a blue spectrum of isocurvature perturbations if the mass of the entropy field perturbation is larger than the Hubble rate. However, the heavy field  $\chi$  is soon suppressed toward the potential valley at  $\chi = 0$ , in which case the correlation between adiabatic and isocurvature perturbations is weak.

Therefore the spectrum of the adiabatic perturbation is typically slightly red-tilted as in the case with  $g = 0$ . In this model we also found an interesting parameter range where large values of  $g$  and  $\chi$  lead to the rather steep red-tilted spectra of strong correlated adiabatic and isocurvature perturbations toward large scales. This comes from the negative mass of the entropy field perturbation with comparable values of two scalar fields.

In the double inflationary scenario motivated by supersymmetric theories, the correlation is found to be very large ( $r_C \simeq 1$ ). This is associated with a tachyonic growth of the entropy field perturbation during the second stage of the double inflation. This strong correlation also yields the mixture of adiabatic and isocurvature perturbations after the symmetry breaking, thereby modifying the spectra of perturbations generated during the first stage of inflation. We found that a variety of power spectra can be obtained by making use of this conversion mechanism.

In the original version of the hybrid inflation with a potential (4.1) [43], the field  $\chi$  is strongly suppressed because of its large effective mass before the symmetry breaking. Inflation ends by a rapid rolling of the field  $\chi$  after the symmetry breaking at  $\phi = \phi_c$ . Since the field  $\chi$  has practically no homogeneous component at  $\phi = \phi_c$ , the decomposition of  $\chi$  between the homogeneous field  $\chi(t)$  and the perturbative part  $\delta\chi(\mathbf{x}, t)$  is not necessarily valid. When  $\chi$  is negligibly small at  $\phi = \phi_c$ , we need to go beyond the perturbation theory using the spatial distribution of the field  $\chi(\mathbf{x}, t)$  as in ref. [59].

Note, however, that in the case of the double inflation the field  $\chi$  is hardly suppressed for  $\phi > \phi_c$  due to the light  $\chi$  mass ( $|\delta| \lesssim 1$ ). Then we are free from the problem of the decomposition of  $\chi$ , in which case our linear analysis can be reliable. We also made some simulations including the back-reaction effect of field fluctuations as the Hartree approximation and obtained similar results as found in this work.

In our work we analyzed two models of the double inflation given by the potentials (3.1) and (4.1). Since these potentials include most of the basic properties of the double inflation, it should be fairly easy to extend our analysis

to other double inflation models motivated by particle physics.<sup>10</sup>

It is really encouraging that double inflation models lead to strong correlations over wide ranges of their parameter spaces. This suggests that searches for correlations in the CMB may yield interesting information and constraints on such models and motivates the development of enhanced slow-roll approximations which can accurately predict the full numerical results.

## ACKNOWLEDGEMENTS

We thank Nicola Bartolo, Christopher Gordon, Julien Lesgourgues, Alexei Starobinsky, Jun'ichi Yokoyama, David Wands, and particularly Carlo Ungarelli, for useful discussions. S.T. is also thankful for financial support from the JSPS (No. 04942). The research of BB is supported under PPARC grant PPA/G/S/2000/00115. D.P. is thankful for financial support from the Monbukagakusho Young Foreign Researcher summer program and grateful to RESCEU for hospitality. S.T. is grateful to Stanislav Alexeyev and Alexey Toporensky for kind hospitality during his stay at the Sternberg Astronomical Institute, Moscow State University.

- 
- [1] J. M. Bardeen, Phys. Rev. D **22**, 1882 (1980); S. Mollerach, Phys. Lett. B **242**, 158 (1990); Phys. Rev. D **42**, 313 (1990); H. Kodama and M. Sasaki, Int. J. Mod. Phys. A **1**, 265 (1986); Int. J. Mod. Phys. A **2**, 491 (1987); J. R. Bond and D. Salopek, Phys. Rev. D **45**, 1139 (1992).
  - [2] V. N. Lukash, Sov. Phys. JETP **52**, 807 (1980); V. F. Mukhanov and G. V. Chibisov, JETP Lett. **33**, 532 (1981); S. W. Hawking, Phys. Lett. **B115**, 295 (1982); A. A. Starobinsky, Phys. Lett. **B117**, 175 (1982); A. H. Guth and S. Y. Pi, Phys. Rev. Lett. **49**, 1110 (1982); J. M. Bardeen, P. J. Steinhardt, and M. S. Turner, Phys. Rev. D **28**, 679 (1983); D. H. Lyth, Phys. Rev. D **31**, 1792 (1985).
  - [3] D. H. Lyth and A. Riotto, Phys. Rept. **314**, 1 (1999) [arXiv:hep-ph/9807278].
  - [4] J. A. Adams, G.G. Ross and S. Sarkar, Nucl. Phys. B **503**, 405 (1997); J. Lesgourgues, Nucl. Phys. B **582**, 593 (2000).
  - [5] A. D. Linde, Phys. Lett. B **158**, 375 (1985); A. A. Starobinsky, JETP Lett. **42**, 152 (1985); L. A. Kofman, Phys. Lett. B **173**, 400 (1986); A. D. Linde and Kofman, Nucl. Phys. B **282**, 555 (1987); D. S. Salopek, Phys. Rev. D **45**, 1139 (1992).
  - [6] H. Kodama and M. Sasaki, Prog. Theor. Phys. Suppl. **78**, 1 (1984).
  - [7] V. F. Mukhanov, H. A. Feldman, and R. H. Brandenberger, Phys. Rep. **215**, 293 (1992).
  - [8] C. Gordon, D. Wands, B. A. Bassett and R. Maartens, Phys. Rev. D **63**, 023506 (2001) [arXiv:astro-ph/0009131].
  - [9] J. c. Hwang and H. Noh, Class. Quant. Grav. **19**, 527 (2002) [arXiv:astro-ph/0103244].
  - [10] L. Amendola, C. Gordon, D. Wands and M. Sasaki, Phys. Rev. Lett. **88**, 211302 (2002) [arXiv:astro-ph/0107089].
  - [11] J. c. Hwang, Astrophys. J. **375**, 443 (1991).
  - [12] W-L. Lee and L-Z. Fang, Europhys. Lett. **56**, 904 (2001).
  - [13] D. Polarski and A. A. Starobinsky, Nucl. Phys. B **385**, 623 (1992).
  - [14] D. Polarski and A. A. Starobinsky, Phys. Rev. D **50**, 6123 (1994) [arXiv:astro-ph/9404061].
  - [15] A. A. Starobinsky and J. Yokoyama, arXiv:gr-qc/9502002.
  - [16] J. Garcia-Bellido and D. Wands, Phys. Rev. D **52**, 6739 (1995) [arXiv:gr-qc/9506050]; J. Garcia-Bellido and D. Wands, Phys. Rev. D **53**, 5437 (1996) [arXiv:astro-ph/9511029].
  - [17] M. Sasaki and E. D. Stewart, Prog. Theor. Phys. **95**, 71 (1996) [arXiv:astro-ph/9507001].
  - [18] A. D. Linde and V. Mukhanov, Phys. Rev. D **56**, 535 (1997) [arXiv:astro-ph/9610219].
  - [19] T. Chiba, N. Sugiyama and J. Yokoyama, Nucl. Phys. B **530**, 304 (1998) [arXiv:gr-qc/9708030].
  - [20] V. F. Mukhanov and P. J. Steinhardt, Phys. Lett. B **422**, 52 (1998) [arXiv:astro-ph/9710038].
  - [21] J. Lesgourgues and D. Polarski, Phys. Rev. D **56**, 6425 (1997) [arXiv:astro-ph/9710083].
  - [22] M. Sasaki and T. Tanaka, Prog. Theor. Phys. **99**, 763 (1998) [arXiv:gr-qc/9801017].
  - [23] Y. Nambu and A. Taruya, Class. Quant. Grav. **15**, 2761 (1998) [arXiv:gr-qc/9801021].
  - [24] D. Langlois, Phys. Rev. D **59**, 123512 (1999).
  - [25] T. Kanazawa, M. Kawasaki, N. Sugiyama and T. Yanagida, Phys. Rev. D **61**, 023517 (2000) [arXiv:hep-ph/9908350].

---

<sup>10</sup>In some models of two-field inflation considered as in refs. [15,28,32], the second stage of inflation is absent. In this case the first consistency relation (2.41) is expected to be valid, while the second one (2.42) may be model-dependent [34].

- [26] D. Langlois and A. Riotto, Phys. Rev. D **62**, 043504 (2000) [arXiv:astro-ph/9912497].
- [27] D. Wands, K. A. Malik, D. H. Lyth and A. R. Liddle, Phys. Rev. D **62**, 043527 (2000) [arXiv:astro-ph/0003278].
- [28] S. Tsujikawa and H. Yajima, Phys. Rev. D **62**, 123512 (2000) [arXiv:hep-ph/0007351].
- [29] J. c. Hwang and H. Noh, Phys. Lett. B **495**, 277 (2000) [arXiv:astro-ph/0009268].
- [30] N. Bartolo, S. Matarrese and A. Riotto, Phys. Rev. D **64**, 083514 (2001) [arXiv:astro-ph/0106022].
- [31] N. Bartolo, S. Matarrese and A. Riotto, Phys. Rev. D **64**, 123504 (2001) [arXiv:astro-ph/0107502].
- [32] A. A. Starobinsky, S. Tsujikawa and J. Yokoyama, Nucl. Phys. B **610**, 383 (2001) [arXiv:astro-ph/0107555].
- [33] S. Groot Nibbelink and B. J. van Tent, Class. Quant. Grav. **19**, 613 (2002) [arXiv:hep-ph/0107272].
- [34] D. Wands, N. Bartolo, S. Matarrese and A. Riotto, Phys. Rev. D **66**, 043520 (2002) [arXiv:astro-ph/0205253].
- [35] D. H. Lyth and D. Wands, Phys. Lett. B **524**, 5 (2002) [arXiv:hep-ph/0110002]; K. Enqvist and M. S. Sloth, Nucl. Phys. B **626**, 395 (2002) [arXiv:hep-ph/0109214]; T. Moroi and T. Takahashi, Phys. Lett. B **522**, 215 (2001) [Erratum-ibid. B **539**, 303 (2002)] [arXiv:hep-ph/0110096]; N. Bartolo and A. R. Liddle, Phys. Rev. D **65**, 121301 (2002) [arXiv:astro-ph/0203076]; T. Moroi and T. Takahashi, arXiv:hep-ph/0206026; D. H. Lyth, C. Ungarelli and D. Wands, arXiv:astro-ph/0208055; M. S. Sloth, arXiv:hep-ph/0208241.
- [36] A. Taruya and Y. Nambu, Phys. Lett. B **428**, 37 (1998) [arXiv:gr-qc/9709035]; B. A. Bassett, D. I. Kaiser and R. Maartens, Phys. Lett. B **455**, 84 (1999) [arXiv:hep-ph/9808404]; F. Finelli and R. H. Brandenberger, Phys. Rev. Lett. **82**, 1362 (1999) [arXiv:hep-ph/9809490]; B. A. Bassett and F. Viniegra, Phys. Rev. D **62**, 043507 (2000) [arXiv:hep-ph/9909353]; F. Finelli and R. H. Brandenberger, Phys. Rev. D **62**, 083502 (2000) [arXiv:hep-ph/0003172]; B. A. Bassett, M. Peloso, L. Sorbo and S. Tsujikawa, Nucl. Phys. B **622**, 393 (2002) [arXiv:hep-ph/0109176]; S. Tsujikawa and B. A. Bassett, Phys. Lett. B **536**, 9 (2002) [arXiv:astro-ph/0204031].
- [37] R. Trotta, A. Riotto and R. Durrer, Phys. Rev. Lett. **87**, 231301 (2001) [arXiv:astro-ph/0104017].
- [38] M. Bucher, K. Moodley and N. Turok, Phys. Rev. D **62**, 083508 (2000) [arXiv:astro-ph/9904231].
- [39] N. Bartolo, S. Matarrese and A. Riotto, Phys. Rev. D **65** (2002) 103505 [arXiv:hep-ph/0112261]; F. Bernardeau and J. P. Uzan, arXiv:hep-ph/0207295; astro-ph/0209330 (2002).
- [40] F. Finelli and R. Brandenberger, Phys. Rev. D **65**, 103522 (2002) [arXiv:hep-th/0112249].
- [41] J. Martin and D. J. Schwarz, Phys. Rev. D **62**, 103520 (2000) [arXiv:astro-ph/9911225].
- [42] S. M. Leach, A. R. Liddle, J. Martin and D. J. Schwarz, Phys. Rev. D **66**, 023515 (2002) [arXiv:astro-ph/0202094].
- [43] A. D. Linde, Phys. Rev. D **49** (1994) 748 [arXiv:astro-ph/9307002].
- [44] E. J. Copeland, A. R. Liddle, D. H. Lyth, E. D. Stewart and D. Wands, Phys. Rev. D **49**, 6410 (1994) [arXiv:astro-ph/9401011].
- [45] L. Randall, M. Soljatic and A. H. Guth, Nucl. Phys. B **472**, 377 (1996); arXiv:hep-ph/9601296.
- [46] G. R. Dvali, Q. Shafi and R. Schaefer, Phys. Rev. Lett. **73**, 1886 (1994) [arXiv:hep-ph/9406319].
- [47] G. G. Ross and S. Sarkar, Nucl. Phys. B **461**, 597 (1996) [arXiv:hep-ph/9506283]; J. A. Adams, G. G. Ross and S. Sarkar, Phys. Lett. B **391**, 271 (1997) [arXiv:hep-ph/9608336].
- [48] R. Jeannerot, Phys. Rev. D **56**, 6205 (1997) [arXiv:hep-ph/9706391].
- [49] E. Halyo, Phys. Lett. B **387**, 43 (1996) [arXiv:hep-ph/9606423]; P. Binetruy and G. R. Dvali, Phys. Lett. B **388**, 241 (1996) [arXiv:hep-ph/9606342].
- [50] C. Panagiotakopoulos, Phys. Rev. D **55**, 7335 (1997) [arXiv:hep-ph/9702433].
- [51] A. D. Linde and A. Riotto, Phys. Rev. D **56**, 1841 (1997) [arXiv:hep-ph/9703209].
- [52] B. A. Bassett, F. Tamburini, D. I. Kaiser and R. Maartens, Nucl. Phys. B **561**, 188 (1999) [arXiv:hep-ph/9901319].
- [53] M. Sasaki, Prog. Theor. Phys. **76**, 1036 (1986); V. F. Mukhanov, Sov. Phys. JETP **68**, 1297 (1988).
- [54] A. A. Starobinsky, JETP Lett. **55** (1992) 489 [Pisma Zh. Eksp. Teor. Fiz. **55** (1992) 477].
- [55] S. M. Leach, M. Sasaki, D. Wands and A. R. Liddle, Phys. Rev. D **64**, 023512 (2001) [arXiv:astro-ph/0101406].
- [56] D. Boyanovsky, D. Cormier, H. J. de Vega, R. Holman and S. P. Kumar, Phys. Rev. D **57**, 2166 (1998) [arXiv:hep-ph/9709232].
- [57] D. Cormier and R. Holman, Phys. Rev. D **60**, 041301 (1999) [arXiv:hep-ph/9812476]; D. Cormier and R. Holman, Phys. Rev. D **62**, 023520 (2000) [arXiv:hep-ph/9912483].
- [58] S. Tsujikawa and T. Torii, Phys. Rev. D **62**, 043505 (2000) [arXiv:hep-ph/9912499]; S. Tsujikawa, Phys. Rev. D **61**, 083516 (2000) [arXiv:hep-ph/0003252].
- [59] G. N. Felder, J. Garcia-Bellido, P. B. Greene, L. Kofman, A. D. Linde and I. Tkachev, Phys. Rev. Lett. **87**, 011601 (2001) [arXiv:hep-ph/0012142]; G. N. Felder, L. Kofman and A. D. Linde, Phys. Rev. D **64**, 123517 (2001) [arXiv:hep-th/0106179].
- [60] M. Bastero-Gil, S. F. King and J. Sanderson, Phys. Rev. D **60**, 103517 (1999) [arXiv:hep-ph/9904315].
- [61] R. Easther and K. i. Maeda, Class. Quant. Grav. **16**, 1637 (1999) [arXiv:gr-qc/9711035].
- [62] J. Garcia-Bellido and A. D. Linde, Phys. Rev. D **57**, 6075 (1998) [arXiv:hep-ph/9711360].